Dual PI3K/mTOR inhibition is required to combat resistance to CDK4/6 inhibitor and endocrine therapy in *PIK3CA*-mutant breast cancer

Carla L. Alves[1,†], Leena Karimi[1,†], Mikkel G. Terp[1¥], Mie K. Jakobsen[1¥], Fiona H. Zhou[2,3], Benedetta Policastro[1], Nikoline Nissen[1], Lene E. Johansen[1], Tina Ravnsborg[4], Leila Eshraghi[2,3], Sana Tamboowala[2,3], Ole N. Jensen[4], Elgene Lim[2,3], Henrik J. Ditzel[1,5,6,*]

[1]Cancer Research Unit, Department of Molecular Medicine, University of Southern Denmark; Odense, Denmark.
[2]Garvan Institute of Medical Research; Darlinghurst, Sydney, NSW, Australia.
[3]St. Vincent's Clinical School, University of New South Wales; Sydney, NSW, Australia.
[4]Department of Biochemistry and Molecular Biology, University of Southern Denmark; Odense, Denmark.
[5]Department of Oncology, Odense University Hospital; Odense, Denmark.
[6]Department of Clinical Research, University of Southern Denmark; Odense, Denmark.

*Corresponding author. Email: hditzel@health.sdu.dk

† These authors contributed equally to this work
¥ These authors contributed equally to this work

One Sentence Summary: Our findings underscore the superior efficacy of gedatolisib compared to alpelisib in preclinical models of *PIK3CA*-mutant ER+ advanced breast cancer.

Abstract

Combined CDK4/6 inhibitor (CDK4/6i) and endocrine therapy (ET) ~~significantly~~ improves outcomes in advanced estrogen receptor positive (ER+) breast cancer, but emergence of resistance to this combination underscores the pressing need for alternative therapeutic strategies. A promising approach involves adding an inhibitor of the PI3K/AKT/mTOR pathway to the standard combined CDK4/6i and ET, but selecting the most effective inhibitors and their optimal combinations has proven to be challenging. Here, we compared the efficacy of various triple combinations utilizing single or dual point PI3K/AKT/mTOR pathway inhibitors in breast cancer cell lines, cell line xenografts, patient-derived xenografts and ~~patient-derived~~ organoids resistant to CDK4/6i and ET, and exhibiting *PIK3CA*, *PTEN* or *AKT1* mutations. Notably, *PIK3CA*-mutant, *PTEN*-wildtype, CDK4/6i- and ET-resistant models, required the addition of the dual PI3K/mTOR inhibitor gedatolisib to effectively impede tumor growth by blocking the HIF-1α pathway through both mTORC1 inhibition and PI3K/AKT-mediated modulation of GSK3αβ activity. Conversely, *PIK3CA*-wildtype, *PTEN*-null cells benefited from triple combinations incorporating either the AKT inhibitor capivasertib or the dual mTORC1/2 inhibitor sapanisertib to block tumor growth. Interestingly, gedatolisib ~~significantly~~ reduced viability of *PIK3CA*- or *AKT1*-mutant and *PTEN*-wildtype CDK4/6i-resistant patient-derived organoids compared to the α-specific PI3K inhibitor alpelisib. Our data support the superiority of gedatolisib over alpelisib in ER+ breast tumors harboring alterations of the PI3K/AKT/mTOR pathway including *PIK3CA*- or *AKT1* mutations.

Keywords: CDK4/6 inhibitor resistance; dual PI3K/mTOR inhibitor; gedatolisib; *PIK3CA*-mutant breast cancer.

Background

CDK4/6 inhibitor (CDK4/6i)-based regimens have revolutionized the treatment paradigm for advanced estrogen receptor-positive (ER+) breast cancer. Currently, three ~~CDK4/6 inhibitors (~~CDK4/6i~~)~~ are approved by both the Food and Drug Administration (FDA) and European Medicines Agency (EMA), namely palbociclib, ribociclib and abemaciclib (*1, 2*). These agents function by inhibiting CDK4 and CDK6, which results in cell cycle arrest and inhibition of tumor growth. By specifically targeting these kinases, CDK4/6i in combination with endocrine therapy (ET) halts the proliferation of cancer cells, thereby impeding disease progression. CDK4/6i are used either in combination with an aromatase inhibitor (AI) as first-line therapy, or together with fulvestrant following progression on ET. All three CDK4/6i have ~~significantly~~ improved progression-free survival (PFS) of patients with advanced ER+ breast cancer. Ribociclib in combination with an AI or fulvestrant has also demonstrated an overall survival (OS) benefit in this patient population, as well as abemaciclib in combination with fulvestrant (*3-5*). Despite the indisputable efficacy of CDK4/6i in combination with ET, the emergence of drug resistance poses a challenge in the long-term management of this disease. Thus, development of novel upfront drug combinations that can delay the emergence of resistance or serve as subsequent treatments following progression on combined CDK4/6i and ET are needed.

Promising strategies include the integration of additional targeted therapies, particularly inhibitors of the PI3K/AKT/mTOR pathway, which controls cancer cell growth, proliferation, and survival. Aberrant activation of this signaling cascade is further linked to resistance to various targeted therapies, including CDK4/6i and ET in ER+ breast cancer (*6-8*). Given the pivotal role of the PI3K/AKT/mTOR pathway in breast cancer progression and drug resistance, numerous inhibitors have been developed to target various nodes of the PI3K/AKT/mTOR pathway. The mTOR inhibitor (mTORi) everolimus was the first to be approved in combination with exemestane in advanced ER+ breast cancer (*9*), however this trial was done prior to the clinical use of CDK4/6i. Presently, there are two *PIK3CA* pathway inhibitors that are FDA approved following progression on an ET in advanced breast cancer. The first, α-specific PI3K inhibitor (PI3Ki) alpelisib, is FDA approved for patients with *PIK3CA*-mutant advanced ER+ breast cancer. Alpelisib plus fulvestrant demonstrated ~~a significant~~ improvement in PFS compared with fulvestrant alone (*10, 11*). The second is the AKT inhibitor (AKTi) capivasertib, which was FDA-approved in combination with fulvestrant for patients with ER+ locally advanced or metastatic breast cancer exhibiting one or more *PIK3CA/AKT1/PTEN*-alterations (*12*). More recently, inavolisib, an α-specific PI3Ki, has also been FDA-approved as first-

line therapy for *PIK3CA*-mutant advanced breast cancer in combination with palbociclib and fulvestrant. This approval is based on the results of the INAVO-120 trial, which demonstrated ~~a significant improvement of~~ prolonged PFS with the triple combination compared to palbociclib and fulvestrant alone, along with a manageable safety profile and a low treatment discontinuation rate (*13*). The FDA has currently granted fast track designation to the dual PI3K/mTOR inhibitor gedatolisib as a treatment for patients with advanced ER+ breast cancer following progression on CDK4/6i plus ET. This designation follows encouraging results from phase 1b dose escalation and expansion clinical trials evaluating triple therapy with gedatolisib, CDK4/6i ~~inhibitor~~ and ET (*14, 15*). Several preclinical and early clinical investigations have shown promising results when combining CDK4/6i with PI3K/AKT/mTOR pathway inhibitors (*7, 16*). It has been observed that CDK4/6i sensitize *PIK3CA*-mutant tumors to PI3Ki, thereby enhancing the efficacy of PI3K blockade. Conversely, mTORC1/2 inhibitors have shown the ability to suppress the growth of CDK4/6i-resistant cells. These findings underscore the potential advantages of combining therapies targeting the ER, CDK4/6 and PI3K/AKT/mTOR pathways in ER+ breast cancer resistant to combined CDK4/6i and ET, as well as potentially using them upfront to delay the development of resistance. Importantly, there is an increasing focus on the clinical development of agents capable of inhibiting multiple points within the PI3K/AKT/mTOR pathway, thus achieving a more complete blockade and bypassing negative feedback loops associated with reduced clinical efficacy. In particular, concurrent inhibition of regulators both upstream and downstream of AKT may prevent its activation subsequent to mTORC1–S6K–IRS1 negative feedback loop inhibition, as observed with mTORC1 blockers.

Here, we assess the efficacy of various triple combinations, comprising dual or single inhibitors of the PI3K/AKT/mTOR pathway, ER degrader (fulvestrant) and CDK4/6i (palbociclib), in preclinical models of ER+ breast cancer resistant to combined CDK4/6i and ET. Our findings demonstrate that *PIK3CA*-mutated, *PTEN*-wildtype, breast cancer cells and patient-derived xenografts (PDXs) resistant to combined CDK4/6i and ET require a triple inhibition approach with a dual pathway inhibitor of the PI3K/AKT/mTOR pathway (gedatolisib) added to standard CDK4/6i and ET to efficiently block tumor growth. In contrast, incorporation of a single α-specific PI3Ki ~~inhibitor~~ (alpelisib) or dual mTORC1/2i (sapanisertib) was not sufficient for long-term tumor growth inhibition. Conversely, *PIK3CA*-wildtype and *PTEN*-null cells benefit from triple combinations including either AKTi or mTORi to efficiently impair tumor growth. Interestingly, patient-derived

organoids (PDOs) *PIK3CA*- or *AKT1*-mutated and *PTEN*-wildtype resistant to CDK4/6i, show ~~significant~~ impairment of viability with gedatolisib, supporting the potential utility of dual PI3K/mTORi in *PTEN*-wildtype breast tumors exhibiting other variations of the PI3K/AKT/mTOR pathway beyond *PIK3CA*-mutations.

Results

Dual PI3K/mTOR inhibition is required for long-term growth inhibition of combined CDK4/6i- and fulvestrant-resistant *PIK3CA*-mutated breast cancer cells.

Previous preclinical studies from our group and others have shown that simply switching the partner of ET from CDK4/6i to a PI3K/AKT/mTOR pathway inhibitor does not efficiently overcome CDK4/6i resistance, and triple-targeting therapies may be required (*6, 17-19*). Additionally, the recent surge in the number and diversity of PI3K/AKT/mTOR inhibitors in clinical development underscores the need for rational approaches to identify biomarkers for selection of patients who may benefit from different PI3K/AKT/mTOR pathway inhibitors.

To determine the most effective triple combination therapy for patients experiencing relapse with combined CDK4/6 inhibition and ET, we compared the efficacy of several single or dual targeted inhibitors of the PI3K/AKT/mTOR pathway. These were administered in combination with the CDK4/6i palbociclib and the ER-degrader fulvestrant in two combined palbociclib- and fulvestrant-resistant cell models of *PIK3CA*-mutant ER+ breast cancer. The combined palbociclib- and fulvestrant-resistant cancer cells were derived from the MCF7 (*PIK3CA*-mutant (p. E545K), *PTEN* and *AKT1*-wildtype) and T47D (*PIK3CA*-mutant (p.H1047R) *PTEN*- and *AKT1*-wildtype) cell lines and named MPF-R and TPF-R, while the corresponding sensitive cells were named M-S and T-S. The single inhibitors of the PI3K/AKT/mTOR pathway that were tested in triple combinations with palbociclib and fulvestrant included alpelisib, an α-specific PI3Ki ~~inhibitor~~ approved for use in combination with ET for advanced ER+ breast cancer (*10*). Additionally, we tested capivasertib, a pan-AKTi ~~inhibitor~~ that has been recently granted approval by the FDA in combination with fulvestrant for advanced ER+ breast cancer based on the results from the CAPItello-291 phase 3 trial (*20*). We also tested the efficacy of the dual mTORC1/C2i sapanisertib and the dual PI3K/mTORi gedatolisib, both of which have shown promising outcomes in early phase clinical trials (*14, 15, 21*). Analysis of the sensitive cells, M-S and T-S showed that all triple combinations ~~significantly~~ impaired cell growth (Fig. 1A-B), viability and proliferation (fig. S1) similar to standard combined palbociclib

and fulvestrant. In contrast, when analyzing the combined palbociclib and fulvestrant resistant MPF-R and TPF-R cells, triple combinations of palbociclib, fulvestrant and alpelisib or gedatolisib were the most effective in inhibiting growth (Fig. 1C-D), viability and proliferation (fig. S1) when compared to standard combined palbociclib and fulvestrant. The growth assay (with crystal violet staining) measures total DNA content but does not differentiate between viable, growth-arrested, or apoptotic cells, while the viability assay (with CellTiter-Blue) assesses metabolic activity, providing a direct measure of cell viability. The proliferation assay (with BrdU incorporation) evaluates DNA synthesis and proliferation rate rather than total cell count or viability. The consistency of results across these complementary assays strengthens the validity of our findings and confirms their robustness across multiple biological endpoints.

Next, we assessed the effect of long-term treatment (12 weeks) with the dual or triple combinations in cells sensitive and resistant to combined fulvestrant and CDK4/6i. All dual and triple combinations were highly and equally effective in preventing outgrowth of resistant colonies in M-S and T-S sensitive cells (Fig. 1E-F). When examining the two combined palbociclib- and fulvestrant-resistant cell lines, the triple combination of gedatolisib, palbociclib and fulvestrant was found to be the most effective in both models ~~(Fig. 1G-H)~~. Importantly, no outgrowth of resistant colonies was observed in MPF-R cells over the entire 12-weeks of treatment with the triple combination of gedatolisib, palbociclib and fulvestrant, while a few resistant colonies appeared with the alpelisib, palbociclib and fulvestrant combination between weeks 10-12 (Fig. 1G). In the TPF-R cells, the triple combination of gedatolisib, palbociclib and fulvestrant was also the most effective treatment combination and prevented the outgrowth of resistant colonies until week 10, while a few resistant colonies appeared with the alpelisib, palbociclib, and fulvestrant combination from week 8 (Fig. 1H).

Analysis of the underlying mechanism of cell growth inhibition by the triple combinations in resistant cells revealed that this effect was not a result of apoptosis induction, as determined by activated caspase-3 mediated fluorescent assay (fig. S2A) and Western blotting analysis of apoptotic markers (fig. S2B). Moreover, all triple combination therapies reduced ~~the protein levels of~~ ER, p-Rb, p-PRAS40 and p-S6 protein expression in both sensitive and resistant cells, indicating efficient blockage of the three signaling pathways; the ER, cyclin D/CDK4-6/Rb, and PI3K/AKT/mTOR pathways (fig. S3A and B). As previously described, the AKTi capivasertib binds to the ATP-binding site of AKT, rendering it catalytically inactive while still allowing hyperphosphorylation at the S473 residue (*22, 23*). Notably, the reduction in p-S6 ~~levels~~ expression, a downstream readout of PI3K/AKT/mTOR pathway activity, was more pronounced with the triple combination including

gedatolisib compared to the other triple combinations and the clinically used double combinations in both MPF-R and TPF-R cells (fig. S3C). Together, these data suggest that dual inhibition of PI3K and mTOR combined with CDK4/6i and fulvestrant is the most effective treatment in inhibiting the PI3K/AKT/mTOR pathway in both ER+ *PIK3CA*-mutant, combined CDK4/6i- and fulvestrant-resistant breast cancer cell models.

AKT and mTOR inhibition effectively blocks growth of combined palbociclib- and fulvestrant-resistant *PIK3CA*-wildtype breast cancer cells.

Next, we evaluated the efficacy of the different drug combinations in another cell line model resistant to combined palbociclib and fulvestrant, ZPF-R, and the corresponding parental sensitive cell line, Z-S, derived from the ZR-75-1 cell line. Unlike the T47D- and MCF7-derived cell line models, ZPF-R does not possess the *PIK3CA* mutation that plays a critical role in the efficacy of the PI3Ki alpelisib, but exhibits loss of *PTEN*. Breast tumors characterized by *PTEN* loss frequently do not respond to either pan-PI3K or isoform-specific PI3K-targeted agents (*24-26*). By assessing the effect of the different drug combinations on the growth and viability of Z-S and ZPF-R, we found that all the triple combinations effectively reduced the growth of the parental Z-S cells, comparable to the effect of the clinically used double combinations (Fig. 2A-D). Conversely, triple combinations of palbociclib, fulvestrant, and capivasertib or sapanisertib were identified as the most effective drug combinations in ZPF-R, and thus differed from that of the *PIK3CA*-mutant resistant cell lines, where the triple combination of gedatolisib, palbociclib and fulvestrant was the most effective. The higher efficacy of inhibitors targeting downstream regulators of the PI3K/AKT/mTOR pathway was confirmed in long-term growth assays with this cell line model (Fig. 2E-F). Overall, these data indicate that direct inhibition of PI3K is required in *PIK3CA*-mutant but not in *PIK3CA*-wildtype, *PTEN*-null breast cancer cells, where blockage of the downstream effectors AKT and mTORC1/2 can be more effective.

Dual blockade of PI3K and mTOR combined with CDK4/6i and ER inhibition is needed to ~~significantly~~ reduce growth of combined palbociclib- and fulvestrant-resistant *PIK3CA*-mutant breast cancer xenografts.

Although our short- and long-term experiments suggested that triple combination with alpelisib was more effective than that with capivasertib, our previous studies have demonstrated that both

inhibitors, when combined with palbociclib and fulvestrant, were highly efficient in inhibiting the growth of ER+ breast cancer resistant to combined palbociclib and fulvestrant (*17, 18*). To directly compare the anticancer activity of these two triple combinations, they were evaluated head-to-head using xenografts of the *PIK3CA*-mutant ER+ breast cancer cell line, MPF-R, which is resistant to combined palbociclib and fulvestrant. For this, MPF-R cells were orthotopically implanted into the mammary fat pad of NOG CIEA mice. Two weeks later, recipient mice were randomized into 2 groups and were treated with fulvestrant and palbociclib combined with either capivasertib or alpelisib. Our results showed that over the 7 weeks of treatment, the tumor volume of mice treated with the triple combination of alpelisib, palbociclib and fulvestrant remained largely the same, while the tumor volume of mice treated with the triple combination of capivasertib, palbociclib and fulvestrant slowly expanded (Fig. 3A). At endpoint, the tumor volume of mice treated with the triple combination of alpelisib, palbociclib and fulvestrant was significantly smaller compared with mice treated with the triple combination of fulvestrant, palbociclib and capivasertib ($P < 0.05$) (Fig. 3B). These findings suggest that alpelisib is more effective than capivasertib when combined with palbociclib and fulvestrant in *PIK3CA*-mutant ER+ breast cancer cells resistant to combined fulvestrant and palbociclib.

Next, we compared the *in vivo* efficacy of the triple combinations with either gedatolisib or alpelisib, which in the long-term growth experiments exhibited the highest effectivity in the *PIK3CA*-mutant fulvestrant- and palbociclib-resistant cells. Similar to the previous in vivo experiment, MPF-R cells were orthotopically implanted into the mammary fat pad of NOG CIEA mice. When the tumors were palpable, mice were randomized into 3 groups and treated with 1) palbociclib and fulvestrant, 2) alpelisib, palbociclib and fulvestrant or 3) gedatolisib, palbociclib and fulvestrant. After 4 weeks of treatment, we found that both triple combinations remained quite effective and significantly reduced the tumor growth compared with the mice treated with combined palbociclib and fulvestrant ($P < 0.0001$, Fig. 3C). Although no statistically significant differences in tumor growth were observed between the two triple combinations at this stage, the triple combination of gedatolisib, palbociclib and fulvestrant resulted in most mice having unpalpable tumors (7/10), while this was not observed for mice receiving the triple combination of alpelisib, palbociclib and fulvestrant. To conduct a more comprehensive evaluation and determine the most effective triple combination, we then analyzed the effectiveness of the two triple combinations by evaluating tumor re-growth after discontinuing treatment. When treatment was discontinued at week 4, mice treated with the triple combination of alpelisib, palbociclib and fulvestrant showed immediate xenograft progression (Fig. 3C). In contrast,

no measurable tumor progression was observed for 2 weeks after the therapy was stopped for the group of mice receiving the triple combination of gedatolisib, palbociclib and fulvestrant. After these 2 weeks, the tumors of the mice treated with the triple combination of gedatolisib, palbociclib and fulvestrant started to regrow, but their size remained generally smaller than those treated with the triple combination including alpelisib (Fig. 3C). Upon resuming the treatments from week 8, where the difference in tumor volume between the 2 groups was not statistically significant, the triple combination of gedatolisib, palbociclib and fulvestrant demonstrated a significant reduction in tumor growth compared to the triple combination of alpelisib, palbociclib, and fulvestrant ($P = 0.0003$, Fig. 3C). Although the control mice, treated initially with palbociclib and fulvestrant, showed rapid tumor expansion in the first 5 weeks, these tumors exhibited rapid shrinkage after initiation of triple therapy with gedatolisib at week 5, reaching a tumor size comparable to that at the starting point of the study after only 3 weeks of treatment with the triple combination. To explore the potential role of cancer stem cells (CSCs) in the differential tumor regrowth upon treatment discontinuation with alpelisib- and gedatolisib-containing combinations, we investigated the expression ~~levels~~ of key CSCs markers after treatment with these 2 triple combinations in the microarray data, however no significant marker differences between the two treatment groups were observed (table S1). This suggests that the differences in tumor regrowth are unlikely to be driven by selective effects on the CSCs population. Collectively, these findings suggest that the triple combination of gedatolisib is superior to triple therapy with alpelisib or capivasertib in abolishing the growth of *PIK3CA*-mutant ER+ tumors resistant to combined palbociclib and fulvestrant in vitro and in vivo.

Dual blockade of PI3K and mTOR combined with CDK4/6i and ER inhibition is needed to ~~significantly~~ reduce growth of combined palbociclib- and fulvestrant-resistant ER+ breast cancer PDX model.

Next, we evaluated the *in vivo* efficacy of the triple combinations with either gedatolisib or alpelisib in an ER+ *PIK3CA*-mutant (p.E542K), *AKT1*- and *PTEN*-wildtype breast cancer PDX model resistant to combined palbociclib and fulvestrant (Gar15-13D-FPR) (*17*). PDX Gar15-13D-FPR tumors treated with palbociclib and fulvestrant (control group) consistently increased tumor growth and reached endpoint (tumor volume 1000 mm^3) after approximately 30 days of treatment (Fig. 4A). Addition of alpelisib to combined palbociclib and fulvestrant blocked tumor growth consistently throughout the treatment period and resulted in markedly smaller tumors compared to the controls ~~(Fig. 4A-C)~~. Notably, the combination gedatolisib, palbociclib and fulvestrant induced tumor

regression after treatment initiation ~~(Fig. 4A-C)~~. This resulted in significantly smaller tumors at endpoint in the tumors treated with gedatolisib- compared to alpelisib-containing combinations (tumor volume $P < 0.0001$; tumor weight $P < 0.001$, Fig. 4B and C). Importantly, 20% of mice of the gedatolisib group had no tumors at the implantation site at the endpoint (Fig. 4~~B~~ D). Furthermore, we found metastases in 22% of mice from the palbociclib and fulvestrant group (spleen) and in 33% of mice from the alpelisib, palbociclib and fulvestrant combination group (spleen and heart), but none in the gedatolisib, palbociclib and fulvestrant combination group. Additionally, weight loss ≥ 15% was comparable in the three treatment groups. These data provide the rationale to incorporate gedatolisib over alpelisib alongside fulvestrant and palbociclib to completely abolish the growth of *PIK3CA*-mutant ER+ tumors resistant to combined palbociclib and fulvestrant *in vitro* and *in vivo*.

Dual PI3K/mTOR inhibitor ~~significantly~~ reduces growth of *PIK3CA*- or *AKT1*-mutant ~~patient-derived organoids~~PDOs resistant to CDK4/6i~~nhibitor~~.

To further validate the efficacy of gedatolisib in clinically relevant models of resistance to CDK4/6i, we evaluated the effect of gedatolisib compared to CDK4/6i in ~~patient-derived~~ breast cancer ~~organoids (~~PDOs exhibiting different sensitivities towards the CDK4/6i abemaciclib (Fig. 5A). PDO-P40 and PDO-P48 exhibited higher IC_{50} to abemaciclib (14.36 and 8.10 µM, respectively) compared to PDO-P46, which showed high sensitivity to this treatment (0.65 µM, Fig. 5A). We observed that gedatolisib was highly effective in both CDK4/6i-resistant PDO-P40 and PDO-P48 (IC_{50}, 0.08 and 0.32 µM, respectively), and also in CDK4/6i-sensitive PDO-P46 (0.10 µM, Fig. 5A). Low concentrations (100 nM) of either abemaciclib or gedatolisib impaired viability of PDO-P46, although the reduction in viability was more pronounced with gedatolisib (fig. S4). Conversely, high concentrations of abemaciclib (10 and 20 µM) were required to inhibit cell viability in PDO-P40 and PDO-P48, while gedatolisib reduced viability of the same organoids in ~~significantly~~ lower concentrations (100 nM) (Fig. 5B and fig. S4). Notably, PDO-P40 is *PIK3CA*- and *PTEN*-wildtype but exhibits *AKT1* hotspot gain-of-function mutation (p.E17K), whereas PDO-P48 is *PIK3CA*-mutant (p.E542K) and *PTEN*- and *AKT1*-wildtype. Consistent with our findings in *PIK3CA*-mutant cells and mice models, gedatolisib showed superiority over alpelisib in reducing organoid viability in PDO-P48 (Fig. 5A and B). These data support the higher efficacy of the dual PI3K/mTOR inhibitor gedatolisib compared to alpelisib in tumors with poor response to CDK4/6i ~~inhibitors~~ with various alterations in the PI3K/AKT/mTOR pathway, such as PDO-P40 and PDO-P48.

Dual PI3K/mTOR inhibitor disrupts HIF-1α signaling and metabolism in *PIK3CA*-mutant ER+ breast cancer cells resistant to combined CDK4/6i and ET.

To provide comprehensive mechanistic insight into the effect of each triple combination, we performed global gene expression analyses in MPF-R cells treated with triple combinations containing either a single PI3Ki (alpelisib), a dual PI3K/mTORi (gedatolisib) or a dual mTORi (sapanisertib), each combined with CDK4/6i and fulvestrant. Gene Set Enrichment Analysis (GSEA) of Hallmark gene sets revealed that while most top altered pathways were broadly similar across the three triple combinations, the combination with the dual PI3K/mTORi uniquely inhibited pathways associated with hypoxia and Notch signaling, an effect not observed with the single PI3Ki or dual mTORi combinations (Fig. 6A and tables S2-S4). This finding is consistent with elevated basal expression ~~level~~ of HIF-1α in MPF-R compared to M-S cells, despite normoxic experimental conditions (fig. S5A) and suggests that the dual PI3K/mTORi effectively abrogates a constitutively active, hypoxia-mimicking transcriptional program in the MPF-R cells. Furthermore, the triple combination with the dual PI3K/mTORi did not induce increased expression of genes associated with the Wnt/β-catenin pathway, as observed with the triple combination containing the single PI3Ki or dual mTORi, or of the EMT pathway, as observed with the dual mTORi treatment only (Fig. 6A and tables S2-S4). These findings suggest a distinct and greater impact of dual PI3K/mTOR inhibition on key oncogenic pathways beyond the canonical PI3K/AKT/mTOR axis.

To further elucidate the functional effects of single and dual-node PI3K/mTORi, we conducted phospho-proteomics on MPF-R cells following treatment with the three triple combinations. Pathway enrichment analysis demonstrated that the dual PI3K/mTORi led to significantly stronger suppression of mTORC1-driven protein synthesis, mTORC2-AKT survival signaling and MAPK-dependent proliferation compared to single PI3Ki ($P < 0.05$, Fig. 6B and table S5). The data also revealed a significant downregulation of phosphorylation ~~levels~~ of proteins involved in the HIF-1α pathway following treatment with triple combination containing dual PI3K/mTORi compared to those with either single PI3Ki or dual mTORi ($P < 0.05$). Particularly, we observed reduced phosphorylation of pyruvate dehydrogenase alpha 1 and 2 (PDHA1/2), which indicates a shift away from glycolysis into oxidative phosphorylation (Fig. 6B, tables S5 and S6). This suggests that the dual PI3K/mTORi combination not only suppresses PI3K/mTOR-driven proliferation but also disrupts HIF-1α-mediated

Warburg-like metabolic phenotype, characterized by a reliance on glycolysis independently of hypoxic conditions.

The gene expression and phospho-proteomics data were validated by Western blot analysis, assessing key regulators of the EMT, Wnt/β-catenin, hypoxia, and Notch pathways following treatment with the three triple combinations or specific siRNA-mediated knockdown of *AKT*, *PIK3CA* and/or *MTOR* (Fig. 6C-E, fig. S5B and C and fig. S6A and B). Although all treatments reduced HIF-1α expression in MPF-R cells, dual siRNA-mediated gene knockdown of *PIK3CA*/*MTOR* showed the most significant decrease in HIF-1α and phospho-GSK3α/β expression ($P < 0.05$ and $P < 0.001$), ~~levels,~~ the latter indicating an increase in GSK3α/β activity (Fig. 6C-E). Furthermore, phospho-PDK1, phospho-TSC2, Snail/Slug, and VEGFA ~~levels~~ expression were also reduced with dual PI3K/mTOR knockdown, though these did not reach statistical significance (fig. S6C and D). Importantly, HIF-1α protein was also decreased in vivo in MPF-R xenografts treated with the triple combination containing the dual PI3K/mTORi compared to those treated with the triple combination containing the single PI3Ki (fig. S7).

Collectively, these findings demonstrate that the dual PI3K/mTORi more effectively blocks constitutively active HIF-1α pathway through both direct mTORC1 inhibition (downstream inhibition), leading to reduced HIF-1α protein synthesis, and PI3K/AKT-mediated modulation of GSK3αβ activity (upstream inhibition), which directly promotes HIF-1α degradation. This combined mechanism leads to overall greater inhibition of the HIF-1α pathway and contributes to a shift in cellular metabolism away from glycolysis (a hallmark of HIF-1α activation and prevalent in resistant cells) and towards oxidative phosphorylation (Fig. 7).

Discussion

CDK4/6i in combination with ET has markedly improved the outcomes of patients with ER+ advanced breast cancer (*27-32*). However, progression on this dual therapy is inevitable, and thus development of novel and optimized therapeutic approaches is urgently needed. Numerous preclinical and clinical studies have underscored the pivotal role of the PI3K/AKT/mTOR pathway in ER+ breast cancer tumorigenesis and treatment response. The integration of a PI3K/AKT/mTOR inhibitor synergistically complements the effects of ET and CDK4/6i, impeding tumor progression and effectively overcoming resistance to treatment (*6, 16, 17, 19, 33*). As a result, there has been a surge in the number and diversity of PI3K/AKT/mTOR inhibitors in clinical development combined with

standard therapy, underscoring the need for a systematic approach to pinpoint the tumors most likely to benefit from a particular inhibitor (*34, 35*).

Previous studies have shown that treatment with a PI3Ki or AKTi after progression on combined CDK4/6i and ET is not sufficient to overcome resistance, and targeting all 3 pathways may be required (*6, 17-19*). To determine the most effective combination therapy targeting the PI3K/AKT/mTOR pathway after progression on combined CDK4/6i and ET, we conducted a comparative analysis of several triple pathway inhibitor combinations, including single or dual targeted inhibitors of the PI3K/AKT/mTOR pathway in combination with CDK4/6i and ET. We tested these combinations using *in vitro* and *in vivo PIK3CA/PTEN*-null and -wildtype ER+ breast cancer cell line models, and in patient-derived breast cancer models including PDXs and PDOs resistant to combined CDK4/6i and ET or CDK4/6i alone. Importantly, we observed that both *PIK3CA/PTEN*-null or -wildtype models resistant to combined CDK4/6i and ET required triplet pathway inhibition with PI3K/AKT/mTOR pathway inhibitors for prolonged tumor suppression compared to standard doublet combinations. These data support the role of triple combination therapies as a rational approach to combat treatment resistance in ER+ metastatic breast cancer (*36*). Indeed, the clinical efficacy of triple inhibition of ER, CDK4/6 and PI3K or mTOR is firmly established (*37*). Recent studies have shown that triple combination of fulvestrant, palbociclib/ribociclib and either capivasertib or alpelisib effectively suppresses tumor growth in models resistant to combined ET and CDK4/6i, while ET in combination with only alpelisib or capivasertib did not (*17, 18*). In addition, replacing the CDK4/6i with an AKT/PI3Ki alongside ET does not prevent tumor outgrowth in resistant models (*17, 18*). It is noteworthy that, dual combinations of fulvestrant with either AKT/PI3Ki or CDK4/6i effectively inhibit the growth of ET and CDK4/6i-sensitive cells, highlighting the need for biomarker-based patient selection for optimizing PI3K/AKT/mTOR inhibitor therapy.

We show that growth inhibition of *PIK3CA*-mutant, *PTEN*-wildtype, combined CDK4/6i- and fulvestrant-resistant cell lines is very efficient with PI3K/AKT/mTOR pathway inhibitors. These induce a more pronounced reduction in key pathway activity markers, including phospho-PRAS40 and phospho-S6 compared to the downstream AKT and mTOR, which may allow for compensatory signaling that sustains pathway activation and less effective disruption of the PI3K/AKT/mTOR pathway. However, dual blockade of PI3K and mTOR is required for prolonged cancer cell growth

inhibition and suppression of outgrowth of resistant colonies. This was further observed *in vivo* using *PIK3CA*-mutant cell line xenografts and PDX models resistant to combined CDK4/6i and fulvestrant. Studies have indicated favorable responses to pan-PI3Ki ~~inhibitors~~ in both *PIK3CA*-mutant and -wildtype tumors (*38, 39*). However, tumors with *AKT* mutations may be more effectively inhibited by dual PI3K/mTOR inhibitors, given their ability to inhibit all isoforms of PI3K and target multiple sites along the pathway, and thus exhibiting the most extensive activity profile, while *PTEN*-null tumors may benefit more from inhibition of the downstream pathway at AKT or mTOR (*40*). This is in line with our findings that CDK4/6i-resistant PDOs harboring *AKT1* mutation, but *PIK3CA*- and *PTEN*-wildtype, showed sensitivity to the dual PI3K/mTORi gedatolisib. Although, isoform-specific PI3Ki ~~inhibitors~~, such as alpelisib, have been preferred in tumors with specific mutations in *PIK3CA*, their efficacy may be diminished in tumors with multiple alterations in the pathway (*41, 42*). We speculate that upregulation of several downstream effectors of PI3K, particularly AKT and PRAS40, observed in our resistant vs. sensitive *PIK3CA*-mutant, *PTEN*-wildtype MCF7 and T47D cells (*17, 18*) may explain the increased efficacy of gedatolisib compared to alpelisib in these cell models. Importantly, our data underscore the diminished efficacy of alpelisib compared to gedatolisib in *PIK3CA*-mutant breast cancer cells, xenografts, PDXs, and PDOs, suggesting a potential role for gedatolisib as a second-line therapy following progression on combined CDK4/6i and fulvestrant. However, this requires validation through randomized clinical trials, which are currently ongoing, comparing gedatolisib to the current standard-of-care second-line therapy, with results eagerly awaited. Importantly, high-p-AKT and/or -PDK-1, and/or low-PTEN ~~levels~~ expression may be used to identify the patient population that will respond poorly to combined CDK4/6i and ET, and that will likely benefit from triple combination as first-line therapy in the advanced setting (*17, 18*) .

Our mechanistic investigations, including global gene expression profiling, phospho-proteomics, and targeted gene knockdown experiments, collectively demonstrate that triple combination containing dual PI3K/mTOR inhibition exhibits superior efficacy in suppressing HIF-1α pathway activity compared to triple combination containing single PI3K or dual mTOR inhibition. The robust reduction in HIF-1α protein expression ~~levels~~ observed with dual PI3K/mTOR inhibition can be primarily attributed to a more comprehensive blockade of the PI3K/AKT/mTOR axis, which effectively circumvents the compensatory feedback loops that often limit the efficacy of single-node inhibitors (*43*). Indeed, our data suggest that the triple combination containing dual PI3K/mTOR inhibitor leads to a more pronounced inhibition of mTORC1-driven HIF-1α protein synthesis (a

downstream effect). Simultaneously, we observe a decrease in the inhibitory phosphorylation, and thus activation, of GSK3α/β (an upstream effect). This activation of GSK3α/β directly contributes to HIF-1α degradation through proteasomal pathways, often in a VHL-independent manner (*44*). This combined downstream and upstream suppression ~~significantly~~ impairs constitutive HIF-1α signaling, thereby reducing its ability to drive tumor growth and glycolytic metabolism, as evidenced by reduced phosphorylation of PDHA1/2, indicating a shift towards oxidative metabolism and a reversal of the Warburg effect typically driven by HIF-1α (*45*).

In contrast to the two *PIK3CA*-mutant combined CDK4/6i- and fulvestrant-resistant models, our findings revealed that triple combinations with either pan- or subunit-specific single or dual point PI3Ki ~~inhibitors~~ did not cause prolonged growth inhibition of *PIK3CA*-wildtype and *PTEN*-null combined CDK4/6i- and fulvestrant-resistant model derived from the ZR-75-1 cell line, and combined therapy with either AKTi or mTORi was required. In *PTEN*-null and *PIK3CA*-wildtype breast cancer cells the PI3K pathway is activated through PIP3 accumulation due to *PTEN* loss, which leads to subsequent AKT activation, making these cells less affected by specific PI3K inhibition (*46*). Indeed, AKTi and mTORi have shown promise for tumors characterized by *PTEN* loss, which typically do not respond to either pan-PI3K or isoform-specific PI3K-targeted agents (*24-26*). In particular, dual mTORC1/2i produce a more complete blockade of mTORC by inhibiting both mTORC1-dependent phosphorylation of S6K1 and mTORC2-dependent phosphorylation of AKT and show activity in *mTORC1*-mutant everolimus-resistant tumors (*47-49*). Based on the rationale that AKT plays a central role in all PI3K signaling activity (*25, 50*), several studies, including our own, have demonstrated sensitivity to AKTi ~~inhibitors~~ in both *PIK3CA*-mutant, *PTEN*-wildtype and *PIK3CA*-wildtype, *PTEN*-null breast cancer cells, with sensitivity correlating with SGK and p-AKT expression ~~levels~~ (*17, 51-53*). This is further supported by the results of CAPitello-291 clinical trial, which demonstrated that the combination of capivasertib and fulvestrant ~~significantly~~ improves PFS compared to fulvestrant alone, and served as the basis for the FDA approval of capivasertib in patients with alterations in *PIK3CA*, *AKT* or *PTEN (54)*. Nevertheless, it has been noted that PI3K controls other independent oncogenic pathways in parallel, such as the ERK signaling, which AKTi may not effectively block (*55*). Consequently, not all *PIK3CA*-mutant breast cancer models may respond to AKTi, as some may stimulate cell growth via an AKT-independent axis, such as PDK1/SGK3/mTORC1 (*52, 56*). This concurs with our *in vitro* and *in vivo* findings wherein triple combination with alpelisib inhibited tumor growth more effectively ~~significantly~~ than triple

combination with the AKTi capivasertib in *PIK3CA*-mutant breast cancer cells and xenograft models resistant to combined CDK4/6i and ET. Importantly, our data suggest that in *PI3KCA*-mutated tumors, which are found in approximately 30-40 % of ER+ advanced breast cancer patients (*57*), the optimal treatment strategy is combining an inhibitor of PI3K (alpelisib or gedatolisib) with a CDK/6i and ET. In *PTEN*-null *PI3KCA*-wildtype tumors, which occur in about 15-30 % of patients (*57*), the optimal therapeutic approach includes combined AKTi (capivasertib) or mTORi (sapanisertib), CDK4/6i, and ET. The co-occurrence of *PIK3CA* mutations and *PTEN* loss is relatively rare, reported in 5-10% of patients (*57*), and in this scenario, either of these triple combinations could be considered, although dual PI3K/mTOR inhibition may provide more complete pathway suppression. Clinical studies evaluating dual PI3K/mTOR inhibitors in patients with *PIK3CA*-mutated and *PTEN*-null tumors are needed to refine therapeutic approaches in this patient population.

It is noteworthy that the effective integration of the PI3K/AKT/mTOR inhibitors into clinical practice depends on determining appropriate dosages that effectively suppress the pathway and show anti-tumor efficacy while demonstrating tolerability. Indeed, the development of compounds aimed at the PI3K/AKT/mTOR pathway has been notably hindered by the extensive toxicity profile of these drugs, particularly metabolic and glucose homoeostasis dysregulation, which are dose-limiting toxicities of both selective and pan PI3Ki ~~inhibitors~~ (*58, 59*). These effects complicate optimization of dosage and treatment schedule for PI3K/AKT/mTOR inhibitors in combination with other pathway inhibitors. Nevertheless, numerous ongoing clinical trials are evaluating multiple drugs targeting the PI3K/AKT/mTOR pathway in different triple combinations in advanced ER+ breast cancer. Recent data from the primary analysis of the phase III INAVO120 trial revealed that the improvement of PFS with the triple combination of inavolisib, palbociclib, and fulvestrant compared with palbociclib and fulvestrant in the first-line advanced breast cancer setting, was accompanied by a manageable toxicity profile (*37*). Similarly, triple combination with gedatolisib, CDK4/6i and ET (fulvestrant or letrozole) was well tolerated, with manageable toxicity and low discontinuation rates due to treatment-related adverse events, in dose escalation and expansion phase 1b studies (*14, 15*). The phase III VIKTORIA-1 study evaluating this triple combination in patients with advanced ER+ breast cancer following progression on combined CDK4/6i and ET is ongoing (clinicaltrials.gov ID NCT05501886) (*60*).

Our study has some limitations. While the mechanistic role of HIF-1α signaling in mediating the antitumor effects of gedatolisib was thoroughly investigated in cell line models, further validation is

needed in more clinically relevant systems, including PDXs and PDOs, and clinical samples from patients receiving triple PI3K/AKT/mTOR-targeted therapies, many of which remain in clinical trials. Furthermore, although we evaluated both single- and dual-node PI3K/AKT/mTOR inhibitors selected for their clinical relevance, emerging agents, such as the PI3Kα-selective inhibitor inavolisib, were not assessed in the context of resistance to combined CDK4/6i and ET. Lastly, the relatively limited number of patient-derived models studied, particularly those representing specific genomic subgroups (*PIK3CA* or *AKT1* mutations, *PTEN* loss), limits the generalizability of our findings across the molecular heterogeneity of ER+ breast cancer.

In summary, we provide evidence that treatment of *PIK3CA*-mutant, *PTEN*-wildtype breast cancer models resistant to combined CDK4/6i and ET require the addition of the dual PI3K/mTORi gedatolisib to standard CDK4/6i and ET to effectively impede tumor growth, whereas incorporation of the *PIK3CA*i alpelisib or dual mTORC1/2i sapanisertib is insufficient for achieving long-term inhibition of tumor growth in these models. Conversely, *PIK3CA*-wildtype and *PTEN*-null cells benefited from triple combinations including either AKTi capivasertib or sapanisertib to efficiently impair tumor growth. Interestingly, *PIK3CA*- or *AKT1*-mutant and *PTEN*-wildtype PDOs resistant to CDK4/6i showed ~~significant~~ growth impairment with gedatolisib, supporting the potential utility of dual PI3K/mTORi in tumors harboring other alterations of the PI3K/AKT/mTOR pathway beyond *PIK3CA*-mutation.

Material and methods

Study design

The main objective of this study was to compare the efficacy of triple combination therapies comprising dual or single inhibitors of the PI3K/AKT/mTOR pathway, CDK4/6i and ET, in models of ER+ breast cancer resistant to CDK4/6i and ET. We employed a multi-model experimental approach using established ER+ breast cancer cell lines, cell line-derived xenografts, PDXs, and PDOs harboring *PIK3CA*, *AKT1*, or *PTEN* alterations. Treatment efficacy was assessed using a range of complementary assays evaluating various aspects of tumor cell growth and viability, ensuring the robustness and reproducibility of our findings. Molecular pathway activation and mechanistic analyses were performed using gene expression profiling, phospho-proteomics, siRNA-mediated gene knockdown, and immunoblotting. All in vivo experiments were conducted with institutional ethical approval, and animals were randomly assigned to treatment groups. Sample sizes were

determined based on prior pilot studies and variance observed in preliminary experiments. No data points or outliers were excluded. Details regarding sample sizes, biological replicates, and statistical methodologies are provided in the corresponding figure legends. All results shown are either representative of, or the mean of, at least two independent biological replicates. Human samples were obtained with informed consent and approved by the institutional ethics committees.

Cell lines and anti-cancer drugs

The original MCF-7 (RRID:CVCL-0031) and T47D (RRID:CVCL-0553) human breast cancer cell lines were obtained from the Breast Cancer Task Force Cell Culture Bank, Mason Research Institute, and the original ZR-75-1 cell line (RRID:CVCL-0588) was obtained from the American Type Culture Collection (ATCC). MCF-7- and T47D-derived combined CDK4/6i palbociclib- and fulvestrant-resistant cell lines MPF-R and TPF-R, respectively, were developed from the original cell lines as previously described (*17*). The original ZR-75-1 cell line was used to establish the fulvestrant-resistant cell line (ZF-R) by long-term treatment with increasing concentrations of fulvestrant) (*17*). ZR-75-1 cells resistant to combined fulvestrant and palbociclib (ZPF-R) were established from fulvestrant-resistant cells by long-term treatment (2 months) with 100 nM fulvestrant and increasing concentrations of palbociclib. Palbociclib concentration was increased weekly by 2-fold, from 10 nM to 160 nM. Sensitive cells grown in parallel with MPF-R, TPF-R and ZPF-R cells were designated M-S, T-S and Z-S, respectively. M-S cells were cultured in phenol red-free Dulbecco's modified Eagle medium (D-MEM)/F-12 (Gibco) supplemented with 1% heat-inactivated fetal bovine serum (FBS, Gibco), 2 mM glutamine (Gibco) and 6 ng/ml insulin (Sigma-Aldrich). MPF-R cells were maintained in the same growth media as M-S supplemented with 200 nM palbociclib and 100 nM fulvestrant. T-S cells were cultured in Roswell Park Memorial Institute (RPMI) 1640 media without phenol red (Gibco), supplemented with 5% FBS, 2 mM glutamine, 8 µg /mL insulin. TPF-R cells were cultured in the same media as T-S and supplemented with 200 mM palbociclib and 100 mM fulvestrant. Z-S cells were routinely propagated in RPMI 1640 medium with phenol red (Gibco) supplemented with 10% FBS, 1% HEPES (Gibco), and 1% Penicillin/Streptomycin (Gibco). ZPF-R cells were maintained in the same growth medium as Z-S cells supplemented with 150 nM palbociclib and 100nM fulvestrant.

Fulvestrant (#1047) was purchased from Tocris (R&D Systems) and dissolved in 96% ethanol. Palbociclib isothiocyanate (#HY-A0065), alpelisib (BYL-719, #HY-15244), abemaciclib (HY-16297A), capivasertib (HY-15431), gedatolisib (#HY-10681) and sapanisertib (HY-13328) were all

purchased from MedchemExpress (Sollentuna, Sweden). Palbociclib was dissolved in water while the other drugs were all dissolved in dimethyl sulfoxide (DMSO, Sigma-Aldrich). All drugs were aliquoted and kept at -20°C.

Cell growth, viability, proliferation, and apoptosis assays

Cells were seeded at a density of 0.125 - 0.5 × 10^4 cells/well in 96-well plates and allowed to adhere for 24 hours. Thereafter, cells were treated with either vehicle or different drug combinations and cell growth was measured using a crystal violet-based colorimetric assay. Absorbance was measured in Paradigm reader (Beckman Coulter) at 570 nm. Cell viability was assessed with CellTiterBlue assay (Promega) according to the manufacturer's instructions. Fluorescence was measured at 560/590 nm in Paradigm reader. Cell proliferation was assessed with the BrdU Cell Proliferation Assay Kit (Cell Signaling Technology) according to the manufacturer's instructions. Apoptotic cell death was determined by activated caspase 3/7-mediated fluorescent assay with Incucyte caspase 3/7 Dye (Sartorius) according to the manufacturer's instructions in a live-cell imaging instrument (IncuCyte S3, Sartorius) at 500/530 nm. Plates were scanned every 2 h in brightfield, phase and green channels using the IncuCyte cell-by-cell scan. Scans were analyzed using the basic analyzer by masking cells and signals for caspase 3/7 green. Green integrated intensity per well relative to phase area confluence was normalized to time 0h and used to generate caspase 3/7 green (apoptosis) curve graphs. Cell outgrowth was assessed as previously described (*18*) by seeding cells at 700-1500 cells per well in 96-well plates (48 wells/treatment) and media with treatment was changed once a week. Positive wells were scored weekly as ≥ 50% confluent by visually inspection by two independent individuals.

siRNA-mediated knockdown

siRNA-mediated knockdown was performed with the lipofectamine 3000 transfection reagent according to the manufacturer's instructions (15282465, ThermoFisher Scientific). Briefly, 0.5*10^6 MPF-R and TPF-R cells were seeded in T25 flasks and incubated at 37 °C for 24 h. Subsequently, cells were transfected with 5.8 nM of the indicated siRNAs. Knockdown efficiency was evaluated by Western blotting of protein lysates collected 120 hours after treatment with siRNAs. The following siRNAs from ThermoFisher were used: *PIK3CA* siRNAs (s10520, GACUAGCUAGAGACAAUGATT ~~and s10521~~), *MTOR* siRNAs (s603, CAUUCGCAUUCAGUCCAUATT ~~and s604~~), *AKT1* siRNAs (s659,

GCGUGACCAUGAACGAGUUTT ~~and s660~~). A nontargeting scrambled (control) siRNA was used as the universal negative control (SIC001, Sigma-Aldrich).

Antibodies and Western blotting

Whole protein lysates were extracted with a radioimmunoprecipitation assay buffer (RIPA) containing 50 mmol/L Tris HCl (pH 8), 150 mmol/L NaCl (pH 8), 1% IgePAL CA-630, 0.5% sodium deoxycholate and 0.1% SDS, along with protease and phosphatase inhibitors (Complete and PhosSTOP, Roche). Protein concentration was determined using the Pierce BCA Protein Assay kit (ThermoFisher Scientific), per manufacturer's instructions. 15-30 µg of whole protein lysate was then loaded onto 4%-20% Mini-PROTEAN TGX Stain-free Protein Gels by Bio-Rad and transferred onto a polyvinylidene fluoride (PVDF) membrane (Bio-Rad). The membranes were blocked using TBS containing 0.1% Tween-20 (Sigma-Aldrich,), and 5% non-fat dry milk powder (Sigma-Aldrich). The membranes were then incubated with primary antibodies overnight at 4°C, followed by incubation with HRP-conjugated secondary antibodies goat anti-rabbit or goat anti-mouse (#P0448 and #P0447, Dako) for 1 hour at room temperature. Immunoreactive bands were detected using the ECL Prime Western Blotting Detection Reagent (GE Healthcare) and visualized on the Chemidoc TM MP imaging system (Bio-Rad). The blots for both the sensitive and resistant cell lines were exposed simultaneously. The primary antibodies listed below were purchased from Cell Signaling Technology: p-Akt S473 (D9E,4060L), Akt (pan) (11E7, 4685), anti-p-Rb Ser780 (3590), Rb (4H1,9309), anti-p-PRAS40 T246 (C77D7, 2997), PRAS40 (D23C7, 2691), anti-p-S6 Ser235/236 (2211), anti-S6 (5G10, 2217), anti-cleaved PARP (9541), anti-PARP (9532), anti-Xiap (2042), anti-BCL2, anti-E-cadherin (3195P), anti-GSK-3a/b (5676), anti-p-GSK-3a/b (9331), anti-Notch 2 (5732), anti-PDK1 (3062), anti-p-PDK1 (3061), anti-TSC2 (3990), anti-p-TSC2 (3611) anti-VEGFA (65373), anti-VEGFB (2463), and anti-HIF-1α (14179). Anti-Epcam (SAB3300054) was obtained from Sigma Aldrich. Anti-SNAIL + Slug (Ab85936) was purchased from Abcam and anti-β-catenin (C19220) from BD Biosciences. Anti-ER (SP1) was purchased from ThermoFisher Scientific and anti-GAPDH (sc-32233) was obtained from Santa Cruz.

Gene expression microarray analysis

MPF-R cells were treated with triple combinations, and after 3 days of treatment, total RNA was extracted and purified with RNeasy Mini kit (Qiagen) per manufacturer´s instructions and arrayed separately in Human Transcriptome Array 2.0 (HTA, Affymetrix, ThermoFisher Scientific). Data

analysis was conducted in Transcriptome Analysis Console software (ThermoFisher Scientific. Gene Set Enrichment Analysis (GSEA 4.3.2) was performed to identify the gene sets enriched in the MPF-R cells following treatment with different triple combinations.

Phospho-proteomics

MPF-R cells were seeded in T175 flasks and treated with different triple combinations. After 72 hours of treatment, cells were harvested in PBS containing Halt protease and phosphatase inhibitor cocktail (ThermoFisher Scientific) using a cell scraper. Subsequently, the cells were washed with PBS containing inhibitors, before the cell pellets were stored in an -80°C freezer until mass spectometry analysis. Cell pellets were resuspended in lysis buffer (50mM ammonium bicarbonate, 1% Sodium Deoxycholate (SDC), 10 mM Dithiothreitol (DTT), 1 x PhosSTOP) and sonicated with a probe sonicator for 3 x 10 sec while kept on ice. Samples were then heated at 80ºC for 10 minutes after which the lysis solution was cleared by spinning at 5000 x g for 10 minutes. Following protein concentration measurement by Nanodrop, 200 µg protein in lysis buffer was subjected to alkylation with 25 mM iodoacetamide (30 minutes, RT, dark) and subsequent quenching with 5 mM DTT. Samples were digested overnight at 37ºC with 5 % Trypsin. SDC was removed from digested samples by precipitation with 2% formic acid (FA) followed by centrifugation at 10,000 g for 5 minutes (*61*). Peptides were desalted on Oasis HLB extraction cartridges (Waters) following the manufactures protocol. The eluate was split in 95% for phospho-enrichment and 5% for proteomics prior to drying by vacuum centrifugation. The proteomics samples were reconstituted in 20 µl 0.1% FA prior to LC-MS. Phosphopeptides were enriched with MagReSyn Zr-IMAC beads (Resyn Biosciences) using a KingFisher Duo Prime instrument (Thermo Fisher Scientific). Phosphopeptides were bound to the beads and washed once in 80% acetonitrile (Acn), 5% trifluoracetic acid (TFA) and 0.1 M Glycolic acid, followed by a second (80% Acn, 1%TFA) and a third wash (10% Acn, 0.2%TFA). Elution was done with 1,25M NH4OH, pH >10, samples were dried and reconstituted in 12 µl 0.1% FA prior to LC-MS (*62*).

LC-MS analysis was done on an Easy nLC coupled in-line to an Exploris 480 Orbitrap mass spectrometer (ThermoFisher Scientific). The 2-column setup comprised a custom-made precolumn (3.5 cm, 100 µm ID, Reprosil Pur 120 C18-AQ, 5 µm (Dr. Maisch)) and a pulled emitter analytical column (18 cm, 75 µm ID, Reprosil Pur 120 C18-AQ, 3 µm (Dr. Maisch)). Solvent A was 0.1% FA and solvent B was 95% Acn, 0.1% FA.

Phospho-proteomics data was acquired by loading 5 µl of the sample on the column and eluting with a gradient of 5% to 25% B in 65 min, 25% to 40% B in 14 min and 40% to 95% B in 1 min. MS was recorded at 120K resolution with a scan rang of m/z 350-1600, the AGC target set to 3e6 and the maximum injection time (IT) set to auto. Tandem MS (MSMS) was done as top 10 at a resolution of 30K with an isolation window of 1.2 m/z, an AGC target of 2e5, an IT of 200 ms and the dynamic exclusion set to 30 s. All MS raw data was searched against the human SwissProt database utilizing the Proteome Discoverer software (ThermoFisher Scientific) with Mascot 3.1 (Matrix Science, UK) as the search engine. Quantitation was done as label-free, employing match between runs and normalization to total peptide amount. With a fragment mass tolerance of 0.05 Da, a precursor mass tolerance of 5 ppm and 2 allowed missed cleavages, a list of 7846 phospho-peptides was obtained for further analysis in R. The R/limma package was used to identify differently abundant phosphor-peptides across the four different treatment conditions (each with three biological replicates). Data were log2-transformed and filtered to retain only phosphor-peptides with at least one condition containing three valid values. Missing values were imputed using a normal distribution-based approach (downshift = 1.8, width = 0.3). After filtration 7167 phospho-peptides were retained for downstream analysis. Differential abundance analysis was carried out using the lmFit function from the R/limma package. Phosphopeptides significantly less abundant (FDR < 0.05), in the gedatolisib treatment group were identified in comparison to the alpelisib and sapanisertib treatment groups~~, applying FDR threshold of 0.05~~. In the differential abundance analysis, 283 phospho-peptides were found to be significantly less abundant (FDR < 0.05) in the gedatolisib treatment group compared to alpelisib, and 43 phosphopeptides were less abundant compared to sapanisertib. ShinyGO (v0.80) was used to perform gene-set enrichment analysis of the significantly downregulated phospho-peptides ($P < 0.05$).

Cell line xenograft studies

1×10^6 MPF-R cells were resuspended in a 1:1 mixture of extracellular matrix (ECM) from Engelbreth-Holm-Swarm sarcoma (Sigma-Aldrich) and D-MEM/F-12 media and implanted orthotopically into the 4th mammary fat pad of 7-week-old female NOG CIEA mice (Taconic) without exogenous estrogen supplements. Following a period of 3 weeks, mice were randomized into three groups and treated with: 1) combined palbociclib (25 mg/kg) and fulvestrant (Faslodex, AstraZeneca, n = 10), 2) triple combination of alpelisib (25 mg/kg), palbociclib and fulvestrant (n = 7), 3) triple combination of gedatolisib (10 mg/kg), palbociclib and fulvestrant (n = 10). Fulvestrant was

formulated at 100 mg/kg in castor oil (Sigma-Aldrich) and administered once a week subcutaneously. Palbociclib and alpelisib were both given via oral gavage 5 days a week and formulated in 25% w/v HPB cyclodextrin (Sigma-Aldrich). Gedatolisib was formulated in 5% w/v HPB cyclodextrin and given by intraperitoneal (IP) injection 5 days a week. Mice in group 1 were treated with combined palbociclib and fulvestrant for 5 weeks and then treated with the triple combination of gedatolisib, palbociclib and fulvestrant for 3 weeks. Mice in groups 2 and 3 underwent treatment for a duration of four weeks, followed by a four-week break (from week 4 to 8) in treatment, before resuming treatment for additional three weeks (from week 8 to 11).

Tumor volumes were measured once a week with calipers and calculated as follows: tumor volume = 0.5 × (length) × (width)2. All animal experiments were performed at the animal core facility at the University of Southern Denmark and animals were housed under pathogen-free conditions with ad libitum food and water.

~~Patient-derived xenograft (~~PDX~~)~~ model

The fulvestrant and palbociclib-resistant PDX model (Gar15-13 FPR) was developed from an ER+, PR- and HER2- tumor with a PIK3CA mutation (p.E542K) Gar15-13 (HREC/16/SVH/29), which was derived from a patient who progressed on aromatase inhibition, as previously described (*17*). The parental PDX was resistant to fulvestrant and responsive to palbociclib. Gar15-13 tumors were chronically exposed to the combination of palbociclib (MedChemExpress) (50 mg/kg, 5 days/week, oral gavage) and fulvestrant (MedChemExpress) (5 mg/body in peanut oil (Sigma-Alrich), SC weekly) over several passages in mice. At each passage, tumors were established to a width of 5 mm before treatment commenced. Growth rates similar to the untreated parental PDX were obtained by the third passage under treatment selection (*63*). For this study, a thawed Gar15-13-FPR PDX-P5 (true P9) was subjected to selection and was harvested when the tumor volume reached 574 mm^3. Sections of 4 mm^3 were implanted into the right 4^{th} inguinal mammary gland of 6–7 week-old female NOD-SCID-IL2γ$R^{-/-}$ mice (Australian BioResources Pty Ltd). When tumor volumes reached between 150-225 mm^3, mice were randomized into three groups and treated with 1) combined palbociclib (25 mg/kg in 25% β-cyclodextran (Sigma-Alrich), 5 days/week, oral gavage) and fulvestrant (2.5 mg/body in peanut oil, SC weekly, n=9); 2) combined palbociclib, fulvestrant and alpelisib (MedChemExpress) (25 mg/kg in 25% β-cyclodextran, 5 days/week, oral gavage, n=10); and 3) combined palbociclib, fulvestrant and gedatolisib (MedChemExpress) (10 mg/kg in 5% β-cyclodextran, 5 days/week, IP, n=10). Tumor volumes were measured twice a week with calipers

until endpoint of tumor volume ≥ 1000 mm^3 or treatment for 30 days were achieved and calculated as: tumor volume = 0.5 x (length) x $(width)^2$. At the end point, 30 days of treatment, tumors were dissected, net weight was obtained using bench top balance and photographed. Tumor sections were fixed in 10% formalin for paraffin embedding and histological staining.

~~Patient-derived organoid (~~PDO~~)~~ studies

Organoids were established from ER+ primary breast cancer as previously described (*64*). Briefly, tumors were mechanically dissociated and enzymatically digested with 1 mg/mL collagenase (Thermofisher) for 1 hour at 37°C in a MACS dissociator (Miltenyi). After dissociation, cells were embedded in 70% cultrex (Bio-techne) in culture media and plated in 15 µL domes in six-well cell culture plates. After 30 minutes incubation at 37°C for solidification of matrix, organoid medium consisting of Advanced DMEM/F12 (ThermoFisher) supplemented with 10 mM HEPES, 1× Glutamax, 1% penicillin/streptomycin, 2% Rspo3-Fc fusion protein conditioned medium (Ipatherapeutics), 1% Noggin-Fc Fusion Protein Conditioned Medium (Ipatherapeutics), 1x B27 Supplement (ThermoFisher), 5 mM Nicotinamide (Sigma Aldrich), 1.25 mM N-acetyl-L-cysteine (Sigma Aldrich), 100 µg/mL Primocin (Invivogen), 5nM Heregulin β1 (PeproTech), 5 ng/mL FGF-7 (PeproTech), 10 ng/mL heat-stable FGF-10 (ThermoFisher), 0.5 µM A83-01 (Tocris Bioscience), 10 ng/mL EGF (PeproTech), 0.5 µM SB202190 (Sigma Aldrich) and 5µM Y-27632 dihydrochloride (AbMole Bioscience). Medium was replenished every 3 to 4 days. Organoids were dissociated using TrypleExpress (Life Technologies) for 15 minutes at 37°C.

Established organoids were plated in 96-well plates embedded in 50% cultrex in culture media (50 µL/well), followed by treatment with serially diluted CDK4/6i ~~inhibitor~~ abemaciclib and dual PI3K/mTOR inhibitor gedatolisib at different concentrations for 1 week. Cell viability was assessed using RealTime-Glo™ MT cell viability assay (Promega) according to the manufacturer's instructions. Luminescence was measured using Paradigm microplate reader (Beckman Coulter) and SoftMax pro 7.0.2 software. Dose-effect curves were generated using GraphPad Prism software (version 8.0).

Statistical analysis

One-way analysis of variance (ANOVA), two-tailed t-test and Mann–Whitney U test were employed, using GraphPad Prism software (GraphPad Software), to determine statistical significance among

data for the *in vitro* and *in vivo* studies as indicated in the figure legends. One-way ANOVA was used for comparison analysis of gene expression under different treatment conditions using TAC software.

List of the Supplementary Materials

Figs. S1 to S7 ~~and~~

Tables S1 to S6

Data File S1

References

1. R. S. Finn, M. Martin, H. S. Rugo, S. Jones, S. A. Im, K. Gelmon, N. Harbeck, O. N. Lipatov, J. M. Walshe, S. Moulder, E. Gauthier, D. R. Lu, S. Randolph, V. Dieras, and D. J. Slamon, Palbociclib and Letrozole in Advanced Breast Cancer. *N Engl J Med* **375**, 1925-1936 (2016).
2. N. C. Turner, J. Ro, F. Andre, S. Loi, S. Verma, H. Iwata, N. Harbeck, S. Loibl, C. Huang Bartlett, K. Zhang, C. Giorgetti, S. Randolph, M. Koehler, M. Cristofanilli, and P. S. Group, Palbociclib in Hormone-Receptor-Positive Advanced Breast Cancer. *N Engl J Med* **373**, 209-19 (2015).
3. M. Piezzo, P. Chiodini, M. Riemma, S. Cocco, R. Caputo, D. Cianniello, G. Di Gioia, V. Di Lauro, F. D. Rella, G. Fusco, G. Iodice, F. Nuzzo, C. Pacilio, M. Pensabene, and M. De Laurentiis, Progression-Free Survival and Overall Survival of CDK 4/6 Inhibitors Plus Endocrine Therapy in Metastatic Breast Cancer: A Systematic Review and Meta-Analysis. *Int J Mol Sci* **21**, (2020).
4. G. N. Hortobagyi, S. M. Stemmer, H. A. Burris, Y. S. Yap, G. S. Sonke, L. Hart, M. Campone, K. Petrakova, E. P. Winer, W. Janni, P. Conte, D. A. Cameron, F. Andre, C. L. Arteaga, J. P. Zarate, A. Chakravartty, T. Taran, F. Le Gac, P. Serra, and J. O'Shaughnessy, Overall Survival with Ribociclib plus Letrozole in Advanced Breast Cancer. *N Engl J Med* **386**, 942-950 (2022).
5. G. W. Sledge, Jr., M. Toi, P. Neven, J. Sohn, K. Inoue, X. Pivot, O. Burdaeva, M. Okera, N. Masuda, P. A. Kaufman, H. Koh, E. M. Grischke, P. Conte, Y. Lu, S. Barriga, K. Hurt, M. Frenzel, S. Johnston, and A. Llombart-Cussac, The Effect of Abemaciclib Plus Fulvestrant on Overall Survival in Hormone Receptor-Positive, ERBB2-Negative Breast Cancer That Progressed on Endocrine Therapy-MONARCH 2: A Randomized Clinical Trial. *JAMA Oncol* **6**, 116-124 (2020).
6. M. T. Herrera-Abreu, M. Palafox, U. Asghar, M. A. Rivas, R. J. Cutts, I. Garcia-Murillas, A. Pearson, M. Guzman, O. Rodriguez, J. Grueso, M. Bellet, J. Cortés, R. Elliott, S. Pancholi, J. Baselga, M. Dowsett, L. A. Martin, N. C. Turner, and V. Serra, Early Adaptation and Acquired Resistance to CDK4/6 Inhibition in Estrogen Receptor-Positive Breast Cancer. *Cancer Res* **76**, 2301-13 (2016).
7. C. Michaloglou, C. Crafter, R. Siersbaek, O. Delpuech, J. O. Curwen, L. S. Carnevalli, A. D. Staniszewska, U. M. Polanska, A. Cheraghchi-Bashi, M. Lawson, I. Chernukhin, R. McEwen, J. S. Carroll, and S. C. Cosulich, Combined Inhibition of mTOR and CDK4/6 Is Required for Optimal Blockade of E2F Function and Long-term Growth Inhibition in Estrogen Receptor-positive Breast Cancer. *Mol Cancer Ther* **17**, 908-920 (2018).
8. D. D. Huang, L. Tang, F. Yang, J. Jin, and X. X. Guan, PIK3CA mutations contribute to fulvestrant resistance in ER-positive breast cancer. *American Journal of Translational Research* **11**, 6055-6065 (2019).
9. J. Baselga, M. Campone, M. Piccart, H. A. Burris, 3rd, H. S. Rugo, T. Sahmoud, S. Noguchi, M. Gnant, K. I. Pritchard, F. Lebrun, J. T. Beck, Y. Ito, D. Yardley, I. Deleu, A. Perez, T. Bachelot, L. Vittori, Z. Xu, P. Mukhopadhyay, D. Lebwohl, and G. N. Hortobagyi, Everolimus in postmenopausal hormone-receptor-positive advanced breast cancer. *N Engl J Med* **366**, 520-9 (2012).

10. F. Andre, E. Ciruelos, G. Rubovszky, M. Campone, S. Loibl, H. S. Rugo, H. Iwata, P. Conte, I. A. Mayer, B. Kaufman, T. Yamashita, Y. S. Lu, K. Inoue, M. Takahashi, Z. Papai, A. S. Longin, D. Mills, C. Wilke, S. Hirawat, D. Juric, and S.-S. Group, Alpelisib for PIK3CA-Mutated, Hormone Receptor-Positive Advanced Breast Cancer. *N Engl J Med* **380**, 1929-1940 (2019).
11. P. Narayan, T. M. Prowell, J. J. Gao, L. L. Fernandes, E. Li, X. Jiang, J. Qiu, J. Fan, P. Song, J. Yu, X. Zhang, B. L. King-Kallimanis, W. Chen, T. K. Ricks, Y. Gong, X. Wang, K. Windsor, S. Y. Rhieu, G. Geiser, A. Banerjee, X. Chen, F. Reyes Turcu, D. K. Chatterjee, A. Pathak, J. Seidman, S. Ghosh, R. Philip, K. B. Goldberg, P. G. Kluetz, S. Tang, L. Amiri-Kordestani, M. R. Theoret, R. Pazdur, and J. A. Beaver, FDA Approval Summary: Alpelisib Plus Fulvestrant for Patients with HR-positive, HER2-negative, PIK3CA-mutated, Advanced or Metastatic Breast Cancer. *Clin Cancer Res* **27**, 1842-1849 (2021).
12. R. H. Jones, A. Casbard, M. Carucci, C. Cox, R. Butler, F. Alchami, T. A. Madden, C. Bale, P. Bezecny, J. Joffe, S. Moon, C. Twelves, R. Venkitaraman, S. Waters, A. Foxley, and S. J. Howell, Fulvestrant plus capivasertib versus placebo after relapse or progression on an aromatase inhibitor in metastatic, oestrogen receptor-positive breast cancer (FAKTION): a multicentre, randomised, controlled, phase 2 trial. *Lancet Oncol* **21**, 345-357 (2020).
13. N. C. Turner, S. A. Im, C. Saura, D. Juric, S. Loibl, K. Kalinsky, P. Schmid, S. Loi, P. Sunpaweravong, A. Musolino, H. Li, Q. Zhang, Z. Nowecki, R. Leung, E. Thanopoulou, N. Shankar, G. Lei, T. J. Stout, K. E. Hutchinson, J. L. Schutzman, C. Song, and K. L. Jhaveri, Inavolisib-Based Therapy in PIK3CA-Mutated Advanced Breast Cancer. *N Engl J Med* **391**, 1584-1596 (2024).
14. R. Layman, R. Wesolowski, H. Han, J. M. Specht, E. M. Stringer-Reasor, E. C. Dees, P. Kabos, I. A. Mayer, U. Vaishampayan, and J. Lu10. *Phase Ib expansion study of gedatolisib in combination with palbociclib and endocrine therapy in women with ER+ advanced breast cancer*. 2021. San Antonio Breast Cancer Symposium.
15. A. Forero-Torres, H. Han, E. C. Dees, R. Wesolowski, A. Bardia, P. Kabos, R. M. Layman, J. M. Lu, K. A. Kern, R. Perea, K. J. Pierce, B. Houk, N. Pathan, and H. S. Rugo, Phase Ib study of gedatolisib in combination with palbociclib and endocrine therapy (ET) in women with estrogen receptor (ER) positive (+) metastatic breast cancer (MBC) (B2151009). *Journal of Clinical Oncology* **36**, 1040-1040 (2018).
16. S. R. Vora, D. Juric, N. Kim, M. Mino-Kenudson, T. Huynh, C. Costa, E. L. Lockerman, S. F. Pollack, M. Liu, X. Li, J. Lehar, M. Wiesmann, M. Wartmann, Y. Chen, Z. A. Cao, M. Pinzon-Ortiz, S. Kim, R. Schlegel, A. Huang, and J. A. Engelman, CDK 4/6 inhibitors sensitize PIK3CA mutant breast cancer to PI3K inhibitors. *Cancer Cell* **26**, 136-49 (2014).
17. C. L. Alves, S. Ehmsen, M. G. Terp, N. Portman, M. Tuttolomondo, O. L. Gammelgaard, M. F. Hundebol, K. Kaminska, L. E. Johansen, M. Bak, G. Honeth, A. Bosch, E. Lim, and H. J. Ditzel, Co-targeting CDK4/6 and AKT with endocrine therapy prevents progression in CDK4/6 inhibitor and endocrine therapy-resistant breast cancer. *Nat Commun* **12**, 5112 (2021).
18. L. Karimi, C. L. Alves, M. G. Terp, M. Tuttolomondo, N. Portman, S. Ehmsen, L. E. Johansen, M. Bak, E. Lim, and H. J. Ditzel, Triple combination targeting PI3K, ER, and CDK4/6 inhibits growth of ER-positive breast cancer resistant to fulvestrant and CDK4/6 or PI3K inhibitor. *Cancer Commun (Lond)* **43**, 720-725 (2023).
19. N. A. O'Brien, M. S. J. McDermott, D. Conklin, T. Luo, R. Ayala, S. Salgar, K. Chau, E. DiTomaso, N. Babbar, F. Su, A. Gaither, S. A. Hurvitz, R. Linnartz, K. Rose, S. Hirawat, and D. J. Slamon, Targeting activated PI3K/mTOR signaling overcomes acquired resistance to CDK4/6-based therapies in preclinical models of hormone receptor-positive breast cancer. *Breast Cancer Res* **22**, 89 (2020).
20. N. C. Turner, M. Oliveira, S. J. Howell, F. Dalenc, J. Cortes, H. L. Gomez Moreno, X. Hu, K. Jhaveri, P. Krivorotko, S. Loibl, S. Morales Murillo, M. Okera, Y. H. Park, J. Sohn, M. Toi, E. Tokunaga, S. Yousef, L. Zhukova, E. C. de Bruin, L. Grinsted, G. Schiavon, A. Foxley, and H. S. Rugo, Capivasertib in Hormone Receptor-Positive Advanced Breast Cancer. *N Engl J Med* **388**, 2058-2070 (2023).
21. J. García-Sáenz, N. Martínez-Jáñez, R. Cubedo, Y. Jerez, A. Lahuerta, S. González-Santiago, N. Ferrer, M. Ramos, J. L. Alonso-Romero, A. Antón, E. Carrasco, J. Chen, R. Neuwirth, K. Galinsky, S. Vincent, E. J.

Leonard, and D. Slamon, Sapanisertib plus Fulvestrant in Postmenopausal Women with Estrogen Receptor-Positive/HER2-Negative Advanced Breast Cancer after Progression on Aromatase Inhibitor. *Clin Cancer Res* **28**, 1107-1116 (2022).
22. R. Ribas, S. Pancholi, S. K. Guest, E. Marangoni, Q. Gao, A. Thuleau, N. Simigdala, U. M. Polanska, H. Campbell, A. Rani, G. Liccardi, S. Johnston, B. R. Davies, M. Dowsett, and L.-A. Martin, AKT Antagonist AZD5363 Influences Estrogen Receptor Function in Endocrine-Resistant Breast Cancer and Synergizes with Fulvestrant (ICI182780) In Vivo. *Molecular Cancer Therapeutics* **14**, 2035-2048 (2015).
23. T. Okuzumi, D. Fiedler, C. Zhang, D. C. Gray, B. Aizenstein, R. Hoffman, and K. M. Shokat, Inhibitor hijacking of Akt activation. *Nat Chem Biol* **5**, 484-93 (2009).
24. T. Sangai, A. Akcakanat, H. Chen, E. Tarco, Y. Wu, K. A. Do, T. W. Miller, C. L. Arteaga, G. B. Mills, A. M. Gonzalez-Angulo, and F. Meric-Bernstam, Biomarkers of response to Akt inhibitor MK-2206 in breast cancer. *Clin Cancer Res* **18**, 5816-28 (2012).
25. B. R. Davies, H. Greenwood, P. Dudley, C. Crafter, D. H. Yu, J. Zhang, J. Li, B. Gao, Q. Ji, J. Maynard, S. A. Ricketts, D. Cross, S. Cosulich, C. C. Chresta, K. Page, J. Yates, C. Lane, R. Watson, R. Luke, D. Ogilvie, and M. Pass, Preclinical pharmacology of AZD5363, an inhibitor of AKT: pharmacodynamics, antitumor activity, and correlation of monotherapy activity with genetic background. *Mol Cancer Ther* **11**, 873-87 (2012).
26. J. Lin, D. Sampath, M. A. Nannini, B. B. Lee, M. Degtyarev, J. Oeh, H. Savage, Z. Guan, R. Hong, R. Kassees, L. B. Lee, T. Risom, S. Gross, B. M. Liederer, H. Koeppen, N. J. Skelton, J. J. Wallin, M. Belvin, E. Punnoose, L. S. Friedman, and K. Lin, Targeting activated Akt with GDC-0068, a novel selective Akt inhibitor that is efficacious in multiple tumor models. *Clin Cancer Res* **19**, 1760-72 (2013).
27. S. A. Im, Y. S. Lu, A. Bardia, N. Harbeck, M. Colleoni, F. Franke, L. Chow, J. Sohn, K. S. Lee, S. Campos-Gomez, R. Villanueva-Vazquez, K. H. Jung, A. Chakravartty, G. Hughes, I. Gounaris, K. Rodriguez-Lorenc, T. Taran, S. Hurvitz, and D. Tripathy, Overall Survival with Ribociclib plus Endocrine Therapy in Breast Cancer. *N Engl J Med* **381**, 307-316 (2019).
28. R. S. Finn, M. Martin, H. S. Rugo, S. Jones, S. A. Im, K. Gelmon, N. Harbeck, O. N. Lipatov, J. M. Walshe, S. Moulder, E. Gauthier, D. R. Lu, S. Randolph, V. Diéras, and D. J. Slamon, Palbociclib and Letrozole in Advanced Breast Cancer. *N Engl J Med* **375**, 1925-1936 (2016).
29. M. Cristofanilli, N. C. Turner, I. Bondarenko, J. Ro, S. A. Im, N. Masuda, M. Colleoni, A. DeMichele, S. Loi, S. Verma, H. Iwata, N. Harbeck, K. Zhang, K. P. Theall, Y. Jiang, C. H. Bartlett, M. Koehler, and D. Slamon, Fulvestrant plus palbociclib versus fulvestrant plus placebo for treatment of hormone-receptor-positive, HER2-negative metastatic breast cancer that progressed on previous endocrine therapy (PALOMA-3): final analysis of the multicentre, double-blind, phase 3 randomised controlled trial. *Lancet Oncol* **17**, 425-439 (2016).
30. G. N. Hortobagyi, S. M. Stemmer, H. A. Burris, Y. S. Yap, G. S. Sonke, S. Paluch-Shimon, M. Campone, K. Petrakova, K. L. Blackwell, E. P. Winer, W. Janni, S. Verma, P. Conte, C. L. Arteaga, D. A. Cameron, S. Mondal, F. Su, M. Miller, M. Elmeliegy, C. Germa, and J. O'Shaughnessy, Updated results from MONALEESA-2, a phase III trial of first-line ribociclib plus letrozole versus placebo plus letrozole in hormone receptor-positive, HER2-negative advanced breast cancer. *Ann Oncol* **29**, 1541-1547 (2018).
31. D. J. Slamon, P. Neven, S. Chia, P. A. Fasching, M. De Laurentiis, S. A. Im, K. Petrakova, G. V. Bianchi, F. J. Esteva, M. Martín, A. Nusch, G. S. Sonke, L. De la Cruz-Merino, J. T. Beck, X. Pivot, G. Vidam, Y. Wang, K. Rodriguez Lorenc, M. Miller, T. Taran, and G. Jerusalem, Phase III Randomized Study of Ribociclib and Fulvestrant in Hormone Receptor-Positive, Human Epidermal Growth Factor Receptor 2-Negative Advanced Breast Cancer: MONALEESA-3. *J Clin Oncol* **36**, 2465-2472 (2018).
32. G. W. Sledge, Jr., M. Toi, P. Neven, J. Sohn, K. Inoue, X. Pivot, O. Burdaeva, M. Okera, N. Masuda, P. A. Kaufman, H. Koh, E. M. Grischke, M. Frenzel, Y. Lin, S. Barriga, I. C. Smith, N. Bourayou, and A. Llombart-Cussac, MONARCH 2: Abemaciclib in Combination With Fulvestrant in Women With

HR+/HER2- Advanced Breast Cancer Who Had Progressed While Receiving Endocrine Therapy. *J Clin Oncol* **35**, 2875-2884 (2017).
33. V. M. Jansen, N. E. Bhola, J. A. Bauer, L. Formisano, K. M. Lee, K. E. Hutchinson, A. K. Witkiewicz, P. D. Moore, M. V. Estrada, V. Sánchez, P. G. Ericsson, M. E. Sanders, P. R. Pohlmann, M. J. Pishvaian, D. A. Riddle, T. C. Dugger, W. Wei, E. S. Knudsen, and C. L. Arteaga, Kinome-Wide RNA Interference Screen Reveals a Role for PDK1 in Acquired Resistance to CDK4/6 Inhibition in ER-Positive Breast Cancer. *Cancer Res* **77**, 2488-2499 (2017).
34. R. Dienstmann, J. Rodon, V. Serra, and J. Tabernero, Picking the point of inhibition: a comparative review of PI3K/AKT/mTOR pathway inhibitors. *Mol Cancer Ther* **13**, 1021-31 (2014).
35. A. S. Clark, I. Makhlin, and A. DeMichele, Setting the Pick: Can PI3K Inhibitors Circumvent CDK4/6 Inhibitor Resistance? *Clin Cancer Res* **27**, 371-373 (2021).
36. N. Pasha and N. C. Turner, Understanding and overcoming tumor heterogeneity in metastatic breast cancer treatment. *Nature Cancer* **2**, 680-692 (2021).
37. S.-A. I. Komal L. Jhaveri, Cristina Saura, Dejan Juric, Sibylle Loibl, Kevin Kalinsky, Peter Schmid, Sherene Loi, , N. S. Eirini Thanopoulou, Guiyuan Lei, Thomas Stout, Katherine E. Hutchinson, Jennifer Schutzman, , and N. C. T. Chunyan Song, *Inavolisib or placebo in combination with palbociclib and fulvestrant in patients with PIK3CA-mutated, hormone receptor-positive, HER2-negative locally advanced or metastatic breast cancer: Phase III INAVO120 primary analysis*, in *San Antonio Breast Cancer Sympoisum*. 2023, SABCS: San Antonio.
38. J. C. Bendell, J. Rodon, H. A. Burris, M. de Jonge, J. Verweij, D. Birle, D. Demanse, S. S. De Buck, Q. C. Ru, M. Peters, M. Goldbrunner, and J. Baselga, Phase I, dose-escalation study of BKM120, an oral pan-Class I PI3K inhibitor, in patients with advanced solid tumors. *J Clin Oncol* **30**, 282-90 (2012).
39. L. W. Cheung, B. T. Hennessy, J. Li, S. Yu, A. P. Myers, B. Djordjevic, Y. Lu, K. Stemke-Hale, M. D. Dyer, F. Zhang, Z. Ju, L. C. Cantley, S. E. Scherer, H. Liang, K. H. Lu, R. R. Broaddus, and G. B. Mills, High frequency of PIK3R1 and PIK3R2 mutations in endometrial cancer elucidates a novel mechanism for regulation of PTEN protein stability. *Cancer Discov* **1**, 170-85 (2011).
40. S. Ogita and P. Lorusso, Targeting phosphatidylinositol 3 kinase (PI3K)-Akt beyond rapalogs. *Target Oncol* **6**, 103-17 (2011).
41. Y. Sun, P. Dey, H. Wu, and B. Leyland-Jones, P110 α-specific inhibitor is more suitable in PIK3CA mutated breast cancer model but ineffective in PTEN loss of function breast cancer model. *Cancer Research* **72**, 2227-2227 (2012).
42. A. Huang, C. Fritsch, C. Wilson, A. Reddy, M. Liu, J. Lehar, C. Quadt, F. Hofmann, and R. Schlegel, Single agent activity of PIK3CA inhibitor BYL719 in a broad cancer cell line panel. *Cancer research* **72**, 3749-3749 (2012).
43. E. Rozengurt, H. P. Soares, and J. Sinnet-Smith, Suppression of feedback loops mediated by PI3K/mTOR induces multiple overactivation of compensatory pathways: an unintended consequence leading to drug resistance. *Mol Cancer Ther* **13**, 2477-88 (2014).
44. D. Flügel, A. Görlach, C. Michiels, and T. Kietzmann, Glycogen synthase kinase 3 phosphorylates hypoxia-inducible factor 1alpha and mediates its destabilization in a VHL-independent manner. *Mol Cell Biol* **27**, 3253-65 (2007).
45. R. Courtnay, D. C. Ngo, N. Malik, K. Ververis, S. M. Tortorella, and T. C. Karagiannis, Cancer metabolism and the Warburg effect: the role of HIF-1 and PI3K. *Mol Biol Rep* **42**, 841-51 (2015).
46. B. D. Manning and L. C. Cantley, AKT/PKB Signaling: Navigating Downstream. *Cell* **129**, 1261-1274 (2007).
47. S. M. Guichard, J. Curwen, T. Bihani, C. M. D'Cruz, J. W. Yates, M. Grondine, Z. Howard, B. R. Davies, G. Bigley, T. Klinowska, K. G. Pike, M. Pass, C. M. Chresta, U. M. Polanska, R. McEwen, O. Delpuech, S. Green, and S. C. Cosulich, AZD2014, an Inhibitor of mTORC1 and mTORC2, Is Highly Effective in ER+ Breast Cancer When Administered Using Intermittent or Continuous Schedules. *Mol Cancer Ther* **14**, 2508-18 (2015).

48. V. S. Rodrik-Outmezguine, M. Okaniwa, Z. Yao, C. J. Novotny, C. McWhirter, A. Banaji, H. Won, W. Wong, M. Berger, E. de Stanchina, D. G. Barratt, S. Cosulich, T. Klinowska, N. Rosen, and K. M. Shokat, Overcoming mTOR resistance mutations with a new-generation mTOR inhibitor. *Nature* **534**, 272-6 (2016).
49. H. A. Burris, 3rd, C. D. Kurkjian, L. Hart, S. Pant, P. B. Murphy, S. F. Jones, R. Neuwirth, C. G. Patel, F. Zohren, and J. R. Infante, TAK-228 (formerly MLN0128), an investigational dual TORC1/2 inhibitor plus paclitaxel, with/without trastuzumab, in patients with advanced solid malignancies. *Cancer Chemother Pharmacol* **80**, 261-273 (2017).
50. C. Costa and A. Bosch, The Strategy of PIKing a Target: What Is AKTually Most Effective? *Clin Cancer Res* **24**, 2029-2031 (2018).
51. E. M. Sommer, H. Dry, D. Cross, S. Guichard, B. R. Davies, and D. R. Alessi, Elevated SGK1 predicts resistance of breast cancer cells to Akt inhibitors. *Biochem J* **452**, 499-508 (2013).
52. P. Castel, H. Ellis, R. Bago, E. Toska, P. Razavi, F. J. Carmona, S. Kannan, C. S. Verma, M. Dickler, S. Chandarlapaty, E. Brogi, D. R. Alessi, J. Baselga, and M. Scaltriti, PDK1-SGK1 Signaling Sustains AKT-Independent mTORC1 Activation and Confers Resistance to PI3Kα Inhibition. *Cancer Cell* **30**, 229-242 (2016).
53. A. Gris-Oliver, M. Palafox, L. Monserrat, F. Brasó-Maristany, A. Òdena, M. Sánchez-Guixé, Y. H. Ibrahim, G. Villacampa, J. Grueso, M. Parés, M. Guzmán, O. Rodríguez, A. Bruna, C. S. Hirst, A. Barnicle, E. C. de Bruin, A. Reddy, G. Schiavon, J. Arribas, G. B. Mills, C. Caldas, R. Dienstmann, A. Prat, P. Nuciforo, P. Razavi, M. Scaltriti, N. C. Turner, C. Saura, B. R. Davies, M. Oliveira, and V. Serra, Genetic Alterations in the PI3K/AKT Pathway and Baseline AKT Activity Define AKT Inhibitor Sensitivity in Breast Cancer Patient-derived Xenografts. *Clin Cancer Res* **26**, 3720-3731 (2020).
54. N. C. Turner, M. Oliveira, S. J. Howell, F. Dalenc, J. Cortes, H. L. G. Moreno, X. Hu, K. Jhaveri, P. Krivorotko, S. Loibl, S. M. Murillo, M. Okera, Y. H. Park, J. Sohn, M. Toi, E. Tokunaga, S. Yousef, L. Zhukova, E. C. d. Bruin, L. Grinsted, G. Schiavon, A. Foxley, and H. S. Rugo, Capivasertib in Hormone Receptor–Positive Advanced Breast Cancer. *New England Journal of Medicine* **388**, 2058-2070 (2023).
55. H. Ebi, C. Costa, A. C. Faber, M. Nishtala, H. Kotani, D. Juric, P. Della Pelle, Y. Song, S. Yano, M. Mino-Kenudson, C. H. Benes, and J. A. Engelman, PI3K regulates MEK/ERK signaling in breast cancer via the Rac-GEF, P-Rex1. *Proc Natl Acad Sci U S A* **110**, 21124-9 (2013).
56. K. M. Vasudevan, D. A. Barbie, M. A. Davies, R. Rabinovsky, C. J. McNear, J. J. Kim, B. T. Hennessy, H. Tseng, P. Pochanard, S. Y. Kim, I. F. Dunn, A. C. Schinzel, P. Sandy, S. Hoersch, Q. Sheng, P. B. Gupta, J. S. Boehm, J. H. Reiling, S. Silver, Y. Lu, K. Stemke-Hale, B. Dutta, C. Joy, A. A. Sahin, A. M. Gonzalez-Angulo, A. Lluch, L. E. Rameh, T. Jacks, D. E. Root, E. S. Lander, G. B. Mills, W. C. Hahn, W. R. Sellers, and L. A. Garraway, AKT-independent signaling downstream of oncogenic PIK3CA mutations in human cancer. *Cancer Cell* **16**, 21-32 (2009).
57. Brigham, W. s. Hospital, H. M. S. C. L. P. P. J. K. R. 13, G. d. a. B. C. o. M. C. C. J. D. L. A. 25, and I. f. S. B. R. S. K. R. B. B. B. B. R. E. T. L. J. T. V. Z. W. S. Ilya, Comprehensive molecular portraits of human breast tumours. *Nature* **490**, 61-70 (2012).
58. A. Esposito, G. Viale, and G. Curigliano, Safety, Tolerability, and Management of Toxic Effects of Phosphatidylinositol 3-Kinase Inhibitor Treatment in Patients With Cancer: A Review. *JAMA Oncol* **5**, 1347-1354 (2019).
59. S. Chia, S. Gandhi, A. A. Joy, S. Edwards, M. Gorr, S. Hopkins, J. Kondejewski, J. P. Ayoub, N. Califaretti, D. Rayson, and S. F. Dent, Novel agents and associated toxicities of inhibitors of the pi3k/Akt/mtor pathway for the treatment of breast cancer. *Curr Oncol* **22**, 33-48 (2015).
60. S. A. Hurvitz, F. Andre, M. Cristofanilli, G. Curigliano, A. Giordano, H. S. Han, M. Martin, B. Pistilli, H. S. Rugo, R. Wesolowski, S. Suzuki, S. Mutka, I. Gorbatchevsky, and S. Loibl, A phase 3 study of gedatolisib plus fulvestrant with and without palbociclib in patients with HR+/ HER2- advanced breast cancer previously treated with a CDK4/6 inhibitor plus a nonsteroidal aromatase inhibitor (VIKTORIA-1). *Journal of Clinical Oncology* **41**, TPS1118-TPS1118 (2023).

61. I. R. León, V. Schwämmle, O. N. Jensen, and R. R. Sprenger, Quantitative assessment of in-solution digestion efficiency identifies optimal protocols for unbiased protein analysis. *Mol Cell Proteomics* **12**, 2992-3005 (2013).
62. I. Arribas Diez, I. Govender, P. Naicker, S. Stoychev, J. Jordaan, and O. N. Jensen, Zirconium(IV)-IMAC Revisited: Improved Performance and Phosphoproteome Coverage by Magnetic Microparticles for Phosphopeptide Affinity Enrichment. *J Proteome Res* **20**, 453-462 (2021).
63. N. Portman, H. H. Milioli, S. Alexandrou, R. Coulson, A. Yong, K. J. Fernandez, K. M. Chia, E. Halilovic, D. Segara, A. Parker, S. Haupt, Y. Haupt, W. D. Tilley, A. Swarbrick, C. E. Caldon, and E. Lim, MDM2 inhibition in combination with endocrine therapy and CDK4/6 inhibition for the treatment of ER-positive breast cancer. *Breast Cancer Res* **22**, 87 (2020).
64. N. Sachs, J. de Ligt, O. Kopper, E. Gogola, G. Bounova, F. Weeber, A. V. Balgobind, K. Wind, A. Gracanin, H. Begthel, J. Korving, R. van Boxtel, A. A. Duarte, D. Lelieveld, A. van Hoeck, R. F. Ernst, F. Blokzijl, I. J. Nijman, M. Hoogstraat, M. van de Ven, D. A. Egan, V. Zinzalla, J. Moll, S. F. Boj, E. E. Voest, L. Wessels, P. J. van Diest, S. Rottenberg, R. G. J. Vries, E. Cuppen, and H. Clevers, A Living Biobank of Breast Cancer Organoids Captures Disease Heterogeneity. *Cell* **172**, 373-386.e10 (2018).

Acknowledgements

We thank Nimmy Geetha for assistance with the PDX experiment, and M Kat Occhipinti for the editorial assistance.

Funding

The study was supported by grants from The Danish Cancer Society, Health Insurance "Denmark", The Region of Southern Denmark Research Council. Proteomics and mass spectrometry research at SDU is supported by the INTEGRA research infrastructure (Novo Nordisk Foundation, grant no. NNF20OC0061575 to O.N.J).

Author contributions

L.K. and C.L.A. contributed equally to the paper. L.K., C.L.A., and H.J.D. conceived the idea. L.K., C.L.A., M.K.J., L.E.J. and L.E. performed cell line, gene and protein experiments. M.G.T., F.Z. and S.T. conducted animal experiments. C.L.A., N.N. and B.P. conducted ~~the patient-derived organoid~~ PDO experiments. T.R. and O.N.J. performed proteomics and phospho-proteomics experiments by mass spectrometry. M.K.J. analyzed phospho-proteomics data. C.L.A., E.L. and H.J.D. reviewed the experimental and data analyses. L.K., C.L.A., and H.J.D. wrote the paper. All authors reviewed the paper.

Competing interests

The authors declare no competing interests.

Data and materials availability

All data associated with this study are in the main article or supplementary materials. The gene expression data generated during the study are publicly available in the gene expression omnibus (GEO) database under the accession number GSE262611. ~~All other datasets generated during the study will be made available upon reasonable request to the corresponding author, Henrik J. Ditzel, email address: hditzel@health.sdu.dk.~~

Ethical considerations

Procedures and endpoints involving laboratory animals were approved by the Experimental Animal Committee of The Danish Ministry of Justice (2021-15-0201-0084) and the Garvan Institute of Medical Research Animal Ethics Committee (protocols 21/10 and 21/11). Patients' samples used to develop PDOs were obtained in accordance with the local legislation and institutional requirements. The study was approved by the Danish Data Protection Agency and the Ethics Committee of the Region of Southern Denmark (approval no S-20230029). The participants provided their written informed consent to participate in this study and samples were coded to maintain patient confidentiality.

Figure legends

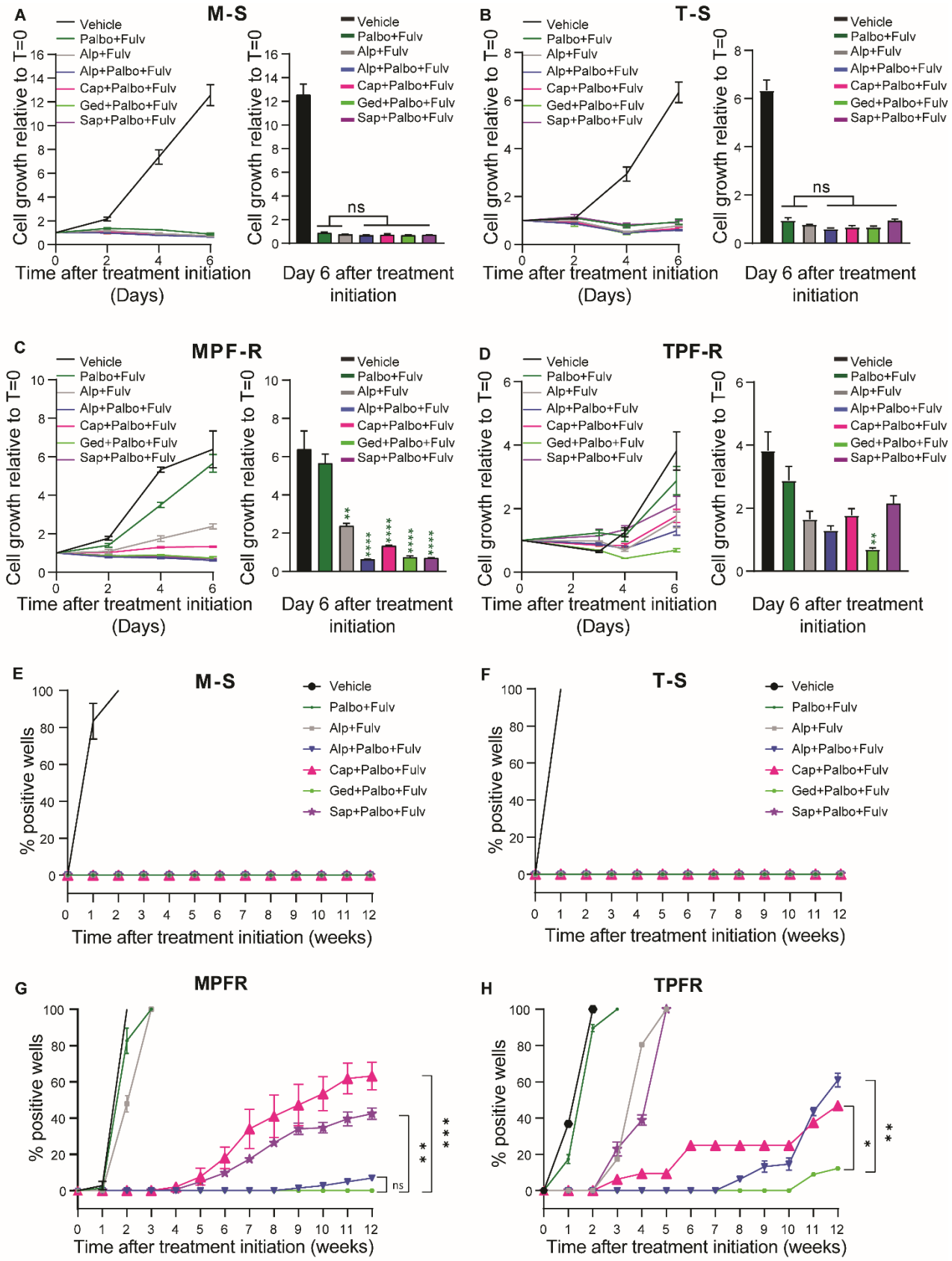
A
M-S
Vehicle
Palbo+Fulv
Alp+Fulv
Alp+Palbo+Fulv
Cap+Palbo+Fulv
Ged+Palbo+Fulv
Sap+Palbo+Fulv
Cell growth relative to T=0
Time after treatment initiation (Days)
ns
Day 6 after treatment initiation
B
T-S
C
MPF-R
D
TPF-R
E
M-S
% positive wells
Time after treatment initiation (weeks)
F
T-S
G
MPFR
H
TPFR

1040

Fig. 1. Combined gedatolisib, palbociclib and fulvestrant are effective in *PIK3CA*-mutant, ER+ breast cancer cells resistant to combined palbociclib and fulvestrant. Combined palbociclib and fulvestrant resistant cells, MPF-R and TPF-R, and the corresponding sensitive cells, M-S and T-S, were treated with different inhibitors of the PI3K/AKT/mTOR pathway including alpelisib (Alp; 1 µM in MS/MPFR and 250-500 nM in T-S/TPF-R), capivasertib (Cap; 250-500 nM in M-S/MPF-R and 100 nM in T-S/TPF-R), sapanisertib (Sap; 10 nM in M-S/MPF-R and 5 nM in TS/TPFR), gedatolisib (Ged; 10 nM) in combination with palbociclib (Palbo; 200 nM) and fulvestrant (Fulv; 100 nM). (**A-D**) Cell growth was evaluated by crystal violet assay over 6 days. The results represent the mean ± SEMs of three biological experiments performed in duplicates shown relative to day 0. For each subfigure, time curves are shown on the left and corresponding endpoint bar graphs on the right. (**E-H**) Outgrowth of resistant colonies were assessed weekly by evaluating the percentage of wells at 50 % or greater confluence (positive wells) over a period of 12 weeks. Statistical analysis using one-way ANOVA was performed on readings at the endpoint to determine significant differences between the treatments (* $P < 0.05$, ** $P < 0.01$ ***, $P < 0.001$ and ****$P < 0.0001$).

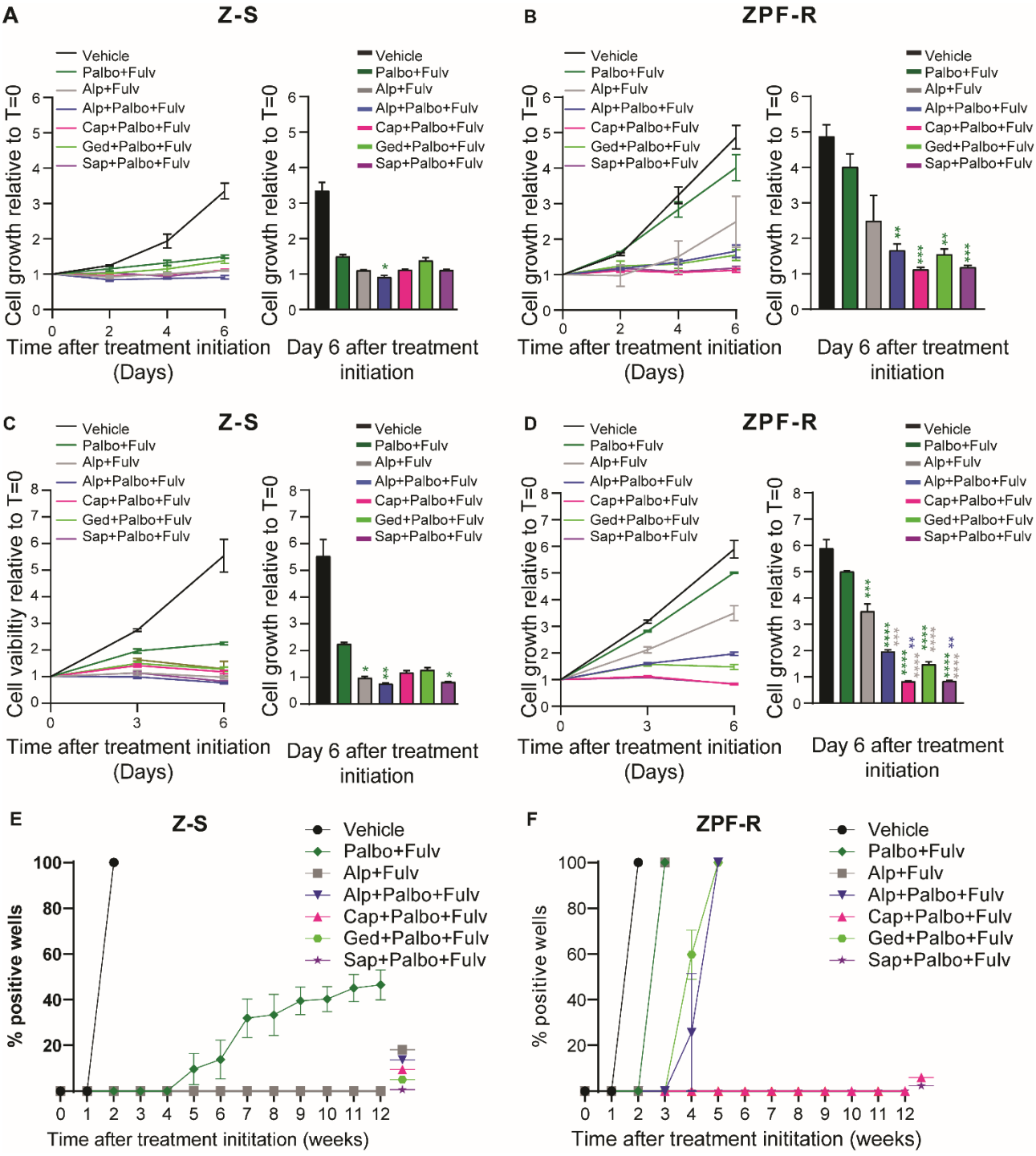

Fig. 2. Combined capivasertib or sapanisertib, palbociclib and fulvestrant is effective in *PIK3CA*-wildtype ER+ breast cancer cells resistant to combined palbociclib and fulvestrant. Combined palbociclib and fulvestrant resistant cells, ZPF-R, and the corresponding sensitive cells, Z-S, were treated with different inhibitors of PI3K/AKT/mTOR including alpelisib (Alp; 6 µM), capivasertib (Cap; 50 nM), sapanisertib (Sap; 5 nM), gedatolisib (Ged; 5 nM) in combination with palbociclib (Palbo; 150 nM) and fulvestrant (Fulv; 100 nM). (**A, B**) Cell growth was evaluated by crystal violet assay over 6 days. (**C, D**) Cell viability was assessed by cell titer-blue assay. The results represent the mean ± SEMs of three biological experiments performed in duplicates and are shown

relative to day 0. For each subfigure, time curves are shown on the left and corresponding endpoint bar graphs on the right. Statistical analysis using one-way ANOVA was performed on readings at day 6 to determine significant differences between the treatments (* $P < 0.05$, ** $P < 0.01$ ***, $P < 0.001$ and ****$P < 0.0001$). (**E, F**) Assessment of the effect of long-term treatment (12 weeks) with dual or triple combinations. Outgrowth of resistant colonies were assessed weekly by evaluating the percentage of wells at 50 % or greater confluence (positive wells) over the treatment period.

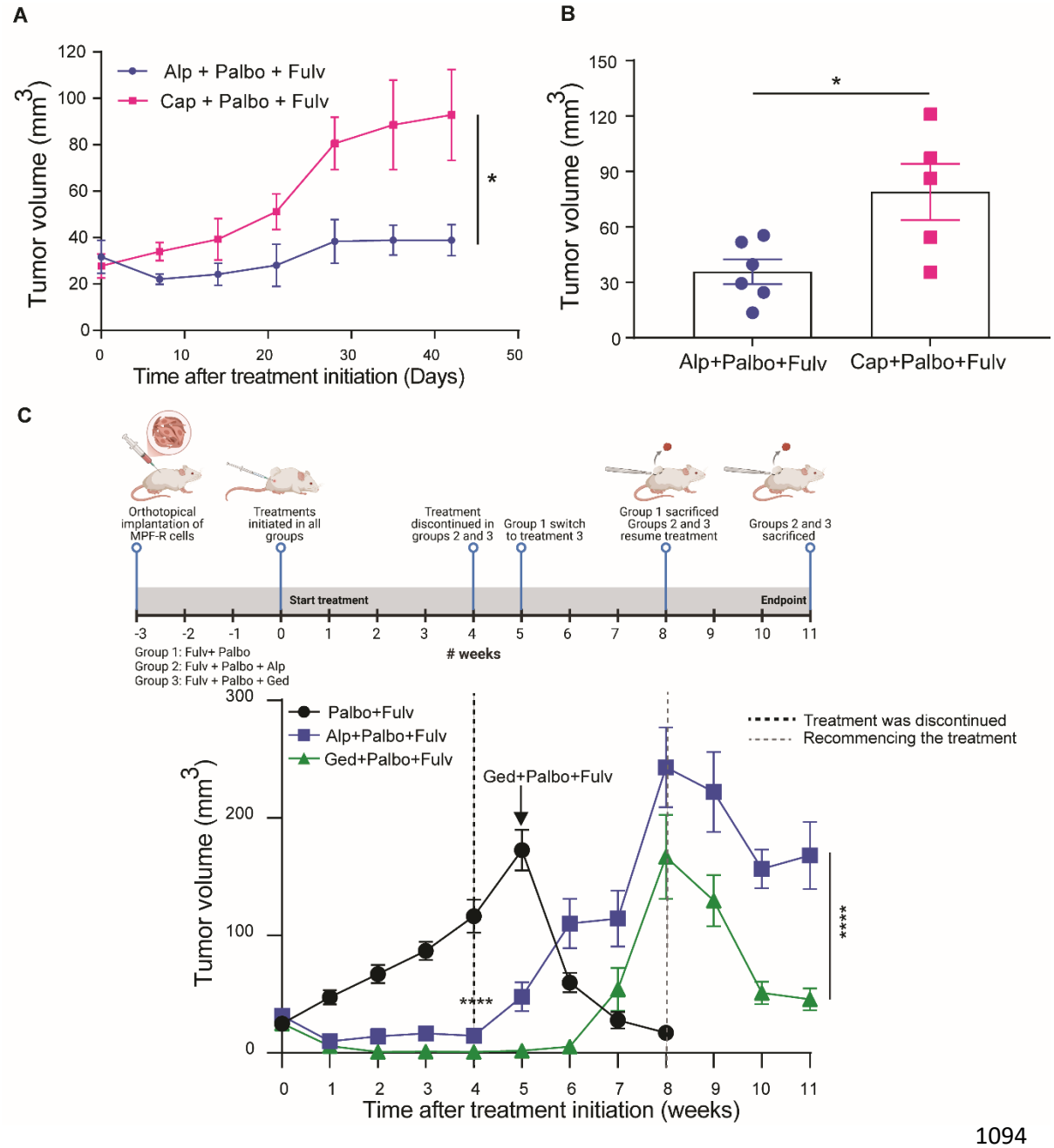

Fig. 3. Triple combination with gedatolisib, palbociclib and fulvestrant effectively inhibits growth of *PIK3CA*-mutant ER+ tumor xenografts resistant to combined palbociclib and fulvestrant. (**A-B**) MPF-R cells ($1x10^6$) resistant to combined palbociclib and fulvestrant were injected into the mammary fat pad of NOG CIEA mice and tumors were allowed to establish for 2

weeks to a size of ≈30 mm^3. Mice were then treated with the combination of fulvestrant (Fulv, 100 mg/kg, SC weekly), palbociclib (Palbo, 25 mg/kg, oral gavage daily) and capivasertib (Cap, 100 mg/kg, oral gavage daily, n= 6) or alpelisib (Alp, 25 mg/kg, oral gavage daily, n = 5). Tumor size was measured weekly. Panel (A) shows the average tumor growth curves measured weekly and panel (B) shows the tumor volumes measured after excision. (**C**) MPF-R cells (1x10^6) were implanted orthotopically into the mammary fat pad of NOG CIEA mice. When tumors were palpable, mice were randomized based on tumor sizes into three groups and treated with; 1) fulvestrant (Fulv, 100 mg/kg, SC. weekly) and palbociclib (palbo, 25 mg/kg, oral gavage daily, n = 10), 2) fulvestrant, palbociclib and alpelisib (Alp, 25 mg/kg, oral gavage daily, n = 7) or 3) fulvestrant, palbociclib and gedatolisib (Ged, 10 mg/kg, IP daily, n = 10). Mice in group 1 initially received combined fulvestrant and palbociclib for 5 weeks, and then combination gedatolisib, palbociclib and fulvestrant was administered for 3 weeks and subsequently sacrificed. In groups 2 and 3, mice received treatment for 4 weeks followed by a 4-week treatment hiatus (week 4 to 8) before resuming the respective treatment for additional 3 weeks (week 8 to 11). Data are shown as mean tumor volume ± SEM. In panel (A-B), significant differences are calculated by two-tailed unpaired t-test (* $P < 0.05$). In panel (C), Significant differences between group 1 and groups 2 and 3 at week 4 were calculated by one-way ANOVA and indicated by asterisks. Significant differences between groups 2 and 3 at the endpoint were calculated by a two-tailed t-test (*$P < 0.05$ and ****$P < 0.0001$).

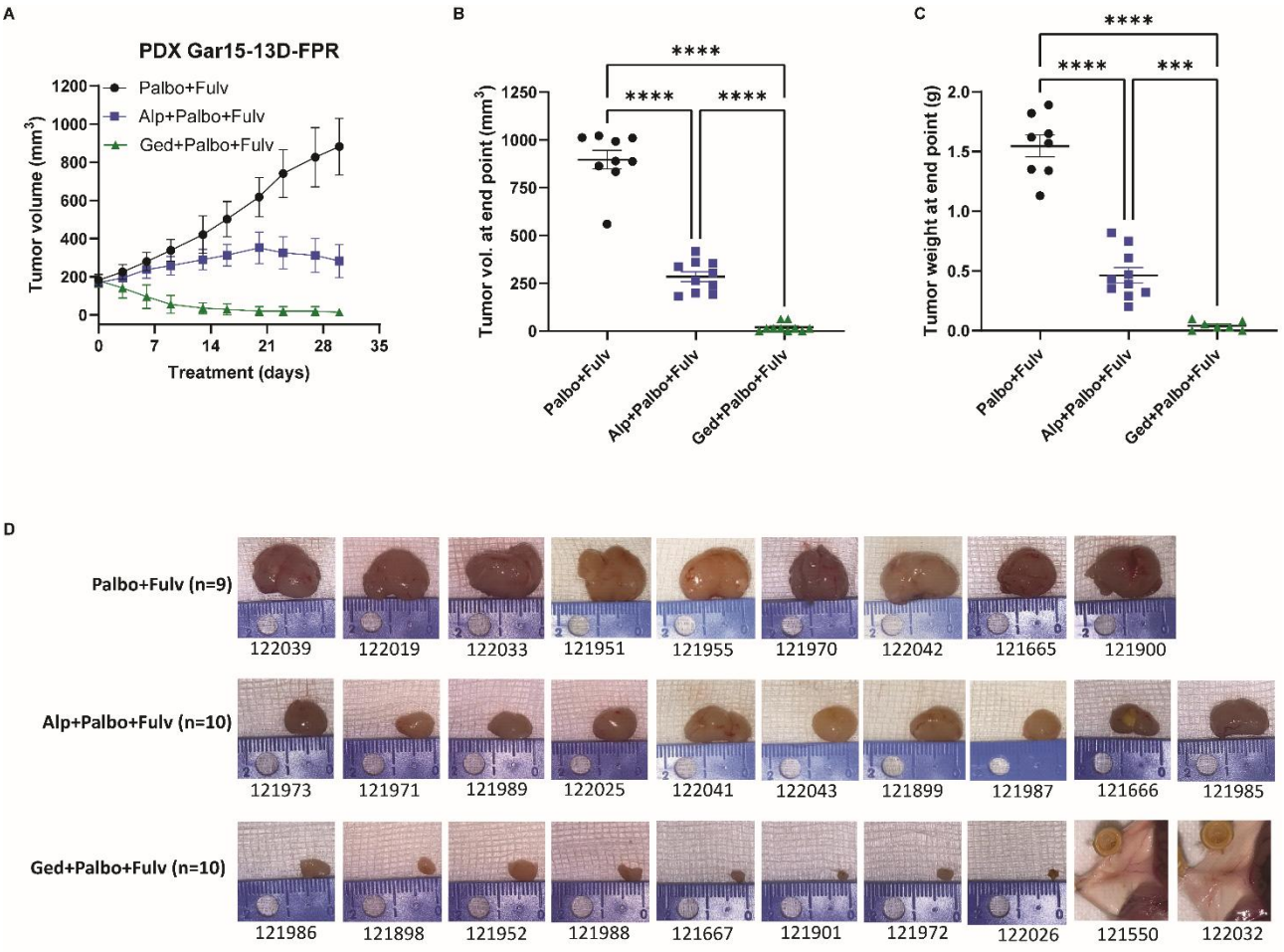

Fig. 4. Combination gedatolisib, palbociclib and fulvestrant induces tumor regression in *PIK3CA*-mutant ER+ breast cancer PDX resistant to combined palbociclib and fulvestrant.

Panel (A) shows average tumor growth curve, panel (B), endpoint tumor volumes (mm3) and (C), endpoint tumor weight (g) from mice bearing the Gar15-13-FPR ~~patient-derived xenograft (~~PDX~~)~~ model resistant to combined palbociclib and fulvestrant treated with: 1) palbociclib (Palbo, 25 mg/kg, 5 days/week, oral gavage) and fulvestrant (Fulv, 100 mg/kg, SC weekly) (n = 9); 2) combination of alpelisib (Alp, 25 mg/kg, 5 days/week, oral gavage), Palbo, and Fulv (n = 10); and 3) combination gedatolisib (Ged, 10 mg/kg, 5 days/week, IP injections), Palbo, and Fulv (n = 10). Tumor size was measured twice weekly for 30 days. Data are presented as mean ± SEM. Significant differences were calculated by one-way ANOVA with Tukey's multiple comparison test (*$P < 0.05$, **$P < 0.01$***, $P < 0.001$, **** $P < 0.0001$) at 30 days. (**D**) Photographs of tumors excised from all mice from each treatment group at endpoint (tumor volume ≥1000 mm^3 or treatment for 30 days). Tumors were not detected in mice 121550 and 122032 treated with combination Ged+Palbo+Fulv.

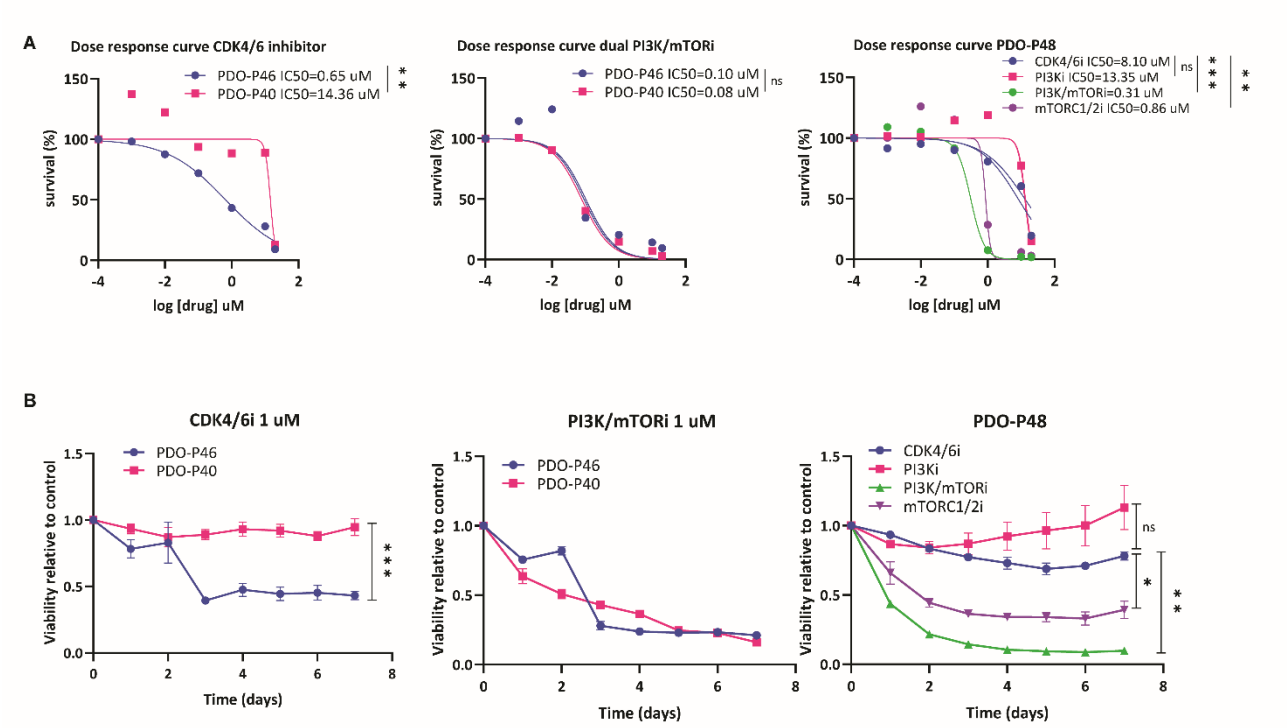

Fig. 5. Dual PI3K/mTOR inhibition efficiently reduced the viability of ER+ *PIK3CA*- or *AKT1*-mutant breast cancer ~~patient-derived organoids~~ PDOs resistant to CDK4/6i. (**A**) Dose-effect curves of CDK4/6i abemaciclib, dual PI3K/mTOR inhibitor gedatolisib, PI3Ki alpelisib and dual mTORC1/2i sapanisertib at day 7 of treatment in three ~~patient-derived~~ breast cancer ~~organoids (~~PDOs~~)~~, PDO-P40, PDO-P46 and PDO-P48, developed from ER+ breast tumors and selected due to their differing IC_{50} towards abemaciclib. (**B**) Effect of 1 µM of abemaciclib, gedatolisib, alpelisib or sapanisertib on viability of PDO-P40, PDO-P46 or PDO-P48 during 7 days of treatment. The results represent the mean ± SEMs of three replicates. Data are presented as mean ± SEM. Significant differences are calculated by one-way ANOVA test (* $P < 0.05$, ** $P < 0.01$ ***, $P < 0.001$).

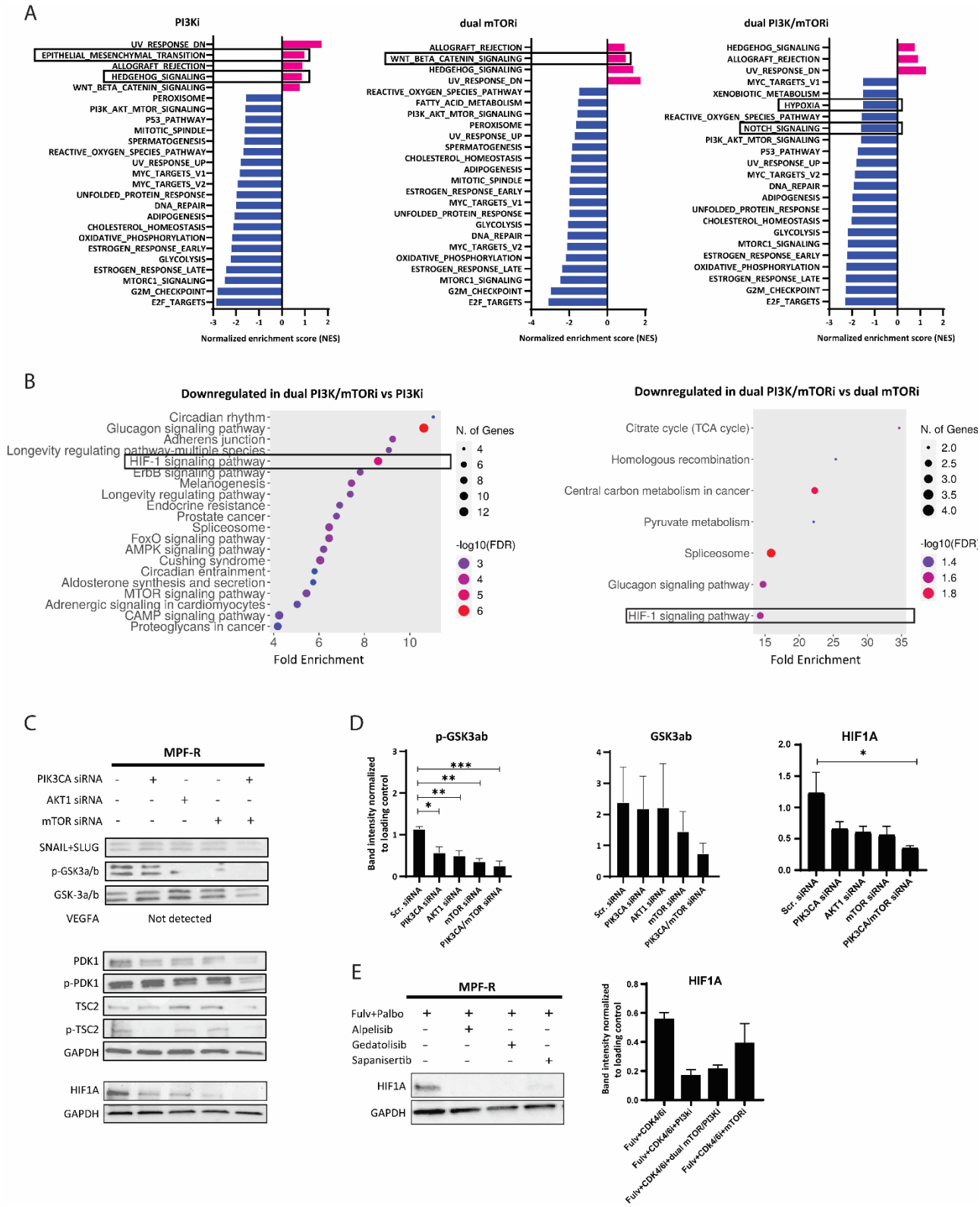

Fig. 6. Combination with gedatolisib, palbociclib and fulvestrant efficiently inhibits the HIF-1α pathway in *PIK3CA*-mutant ER+ breast cancer resistant to combined CDK4/6i and ET. (A) Gene set enrichment analysis of gene expression data in MPF-R cells untreated vs. treated with combinations including fulvestrant, palbociclib, and alpelisib (single PI3Ki), or gedatolisib (dual

PI3K/mTORi) or sapanisertib (dual mTORi). **(B)** Pathway analysis of phospho-proteomics data in MPF-R cells treated with combinations with the dual PI3K/mTORi compared to single PI3Ki or dual mTORi. Three biological replicates were used. Western blot analysis of HIF-1α and GSK3αβ in MPF-R cells after 3 days of exposure to (C, D) siRNA targeting *AKT*, *PIK3CA* or/and *MTOR* or (E) the three drug combinations. GAPDH was used as a loading control. Densitometry analysis of Western blot bands was performed using Image Lab ~~ImageJ~~ software from BioRad. Data are shown as the area under the curve (AUC) normalized to loading control. Data are presented as mean ± SEM. Significant differences are calculated by one-way ANOVA test (* $P < 0.05$, ** $P < 0.01$ ***, $P < 0.001$). For comparisons where no asterisks are indicated, no statistically significant differences were observed.

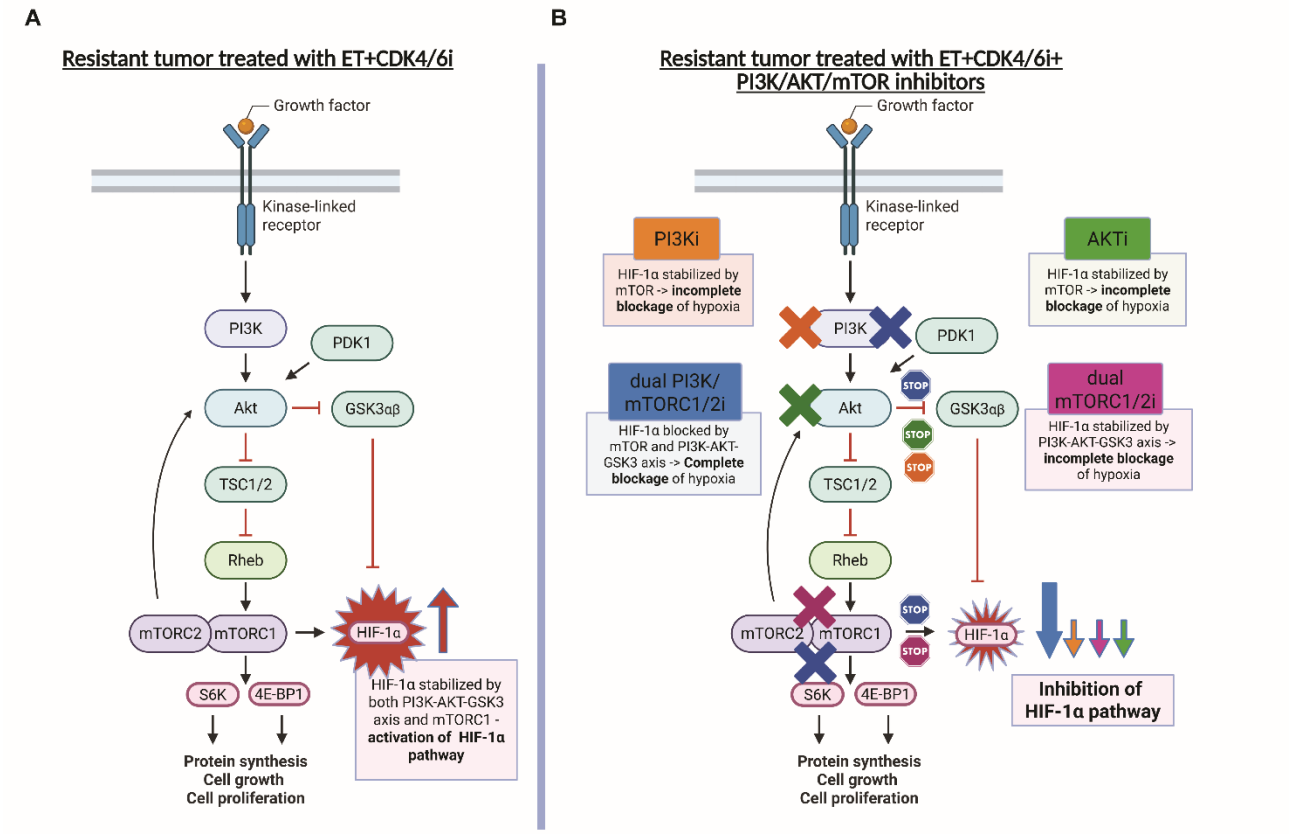

Fig. 7. Proposed mechanistic model illustrating the effect of single or dual-node PI3K/AKT/mTOR inhibitors on constitutive HIF-1α signaling. (A) Combined CDK4/6i and fulvestrant resistant tumors exhibit activation of the PI3K/AKT/mTOR pathway which drives high basal HIF-1α expression ~~levels~~. This occurs through two main mechanisms: mTORC1-mediated increase in HIF-1α protein synthesis, and PI3K/AKT-mediated inhibition of GSK3αβ which reduces HIF-1α degradation. This combined stabilization and activation of HIF-1α promotes a glycolytic (Warburg-like) metabolism ultimately contributing to tumor growth and survival. **(B)** Treatment with a single PI3Ki (alpelisib) primarily inhibits HIF-1α through upstream modulation of GSK3αβ activity via the PI3K/AKT axis, but does not fully suppress mTORC1-driven HIF-1α synthesis. Conversely, a dual mTORi (sapanisertib) predominantly inhibits HIF-1α via mTORC1 (downstream effects on protein synthesis), leaving the PI3K/AKT-GSK3αβ pathway largely unaffected. A dual PI3K/mTORi (gedatolisib) effectively blocks HIF-1α activation through both PI3K/AKT-GSK3αβ-mediated

degradation and mTORC1-mediated protein synthesis, leading to a more profound reduction in HIF-1α activity and greater impairment of tumor growth and survival.

Supplementary Figures

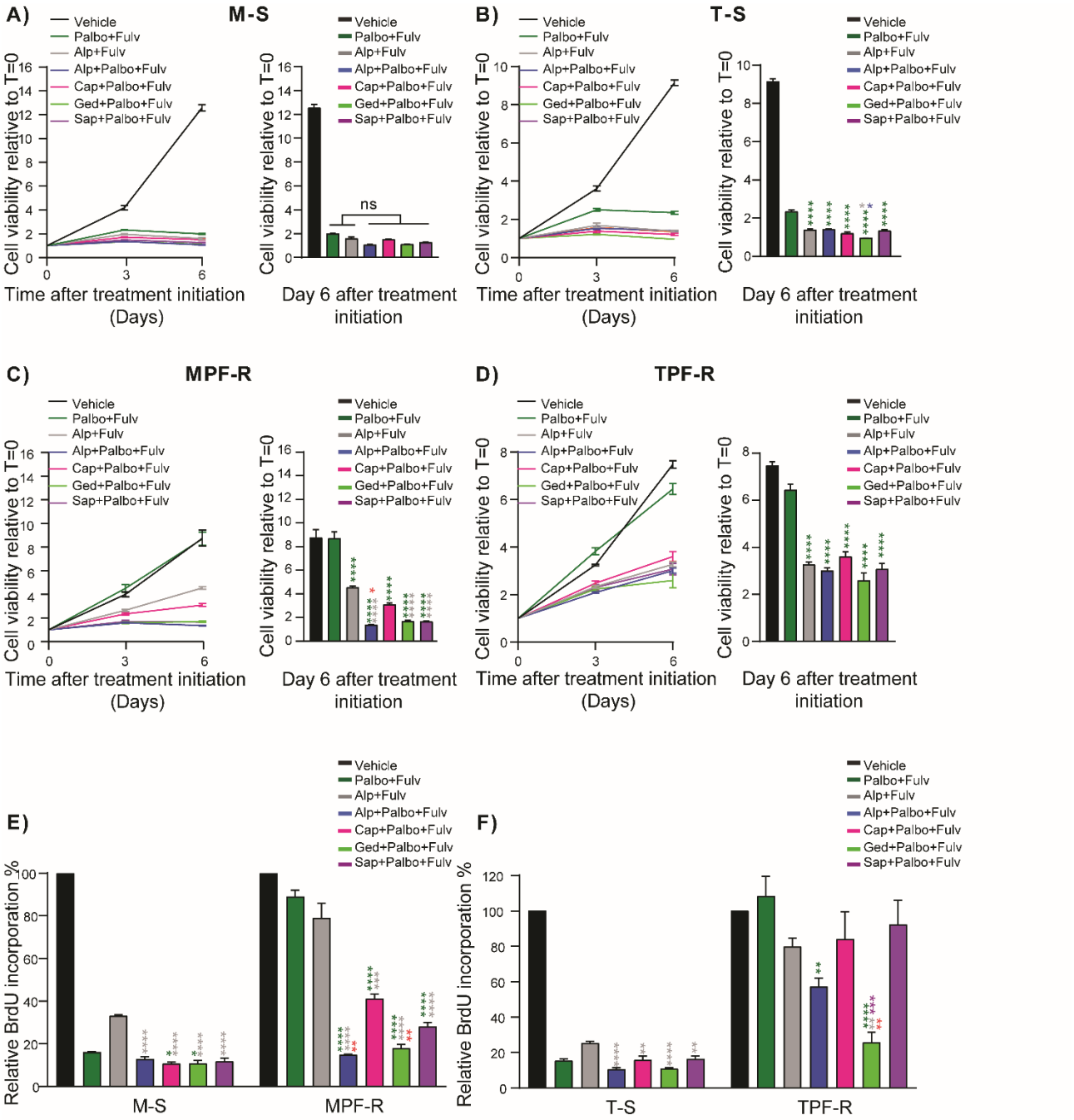

Supplementary Figure S1. Triple targeting of the PI3K/AKT/mTOR, cyclin D/CDK4-6/Rb and ER pathways reduces viability and proliferation of ER+ breast cancer cells resistant to combined palbociclib and fulvestrant. Combined palbociclib and fulvestrant-resistant cells, MPF-R and TPF-R, and the corresponding sensitive cells, M-S and T-S, were treated with different inhibitors of the PI3K/AKT/mTOR pathway including alpelisib (Alp: 1 µM in MS/MPFR and 250-500 nM in T-S/TPF-R), capivasertib (Cap; 250-500 nM in M-S/MPF-R and 100 nM in T-S/TPF-R), sapanisertib (Sap; 10 nM in M-S/MPF-R and 5 nM in TS/TPFR), gedatolisib (Ged; 10 nM) in combination with palbociclib (Palbo; 200 nM) and fulvestrant (Fulv; 100 nM). **A-D)**. The CellTiter-blue cell assay was conducted over 6 days to evaluate cell viability. The results

are shown relative to day 0 and presented as mean ± SEMs of three biological experiments conducted in duplicates. Each subfigure displays time curves on the left and corresponding endpoint bar graphs on the right. Statistical analysis was performed on data at day 6 to determine significant differences between the treatments. **E-F)** BrdU incorporation assay was performed after 6 days of treatment in three biological replicates and data are shown as mean ± SEMs. Statistical significance was calculated by one-way ANOVA (* $P < 0.05$, ** $P < 0.01$, ***$P < 0.001$, and **** $P < 0.0001$).

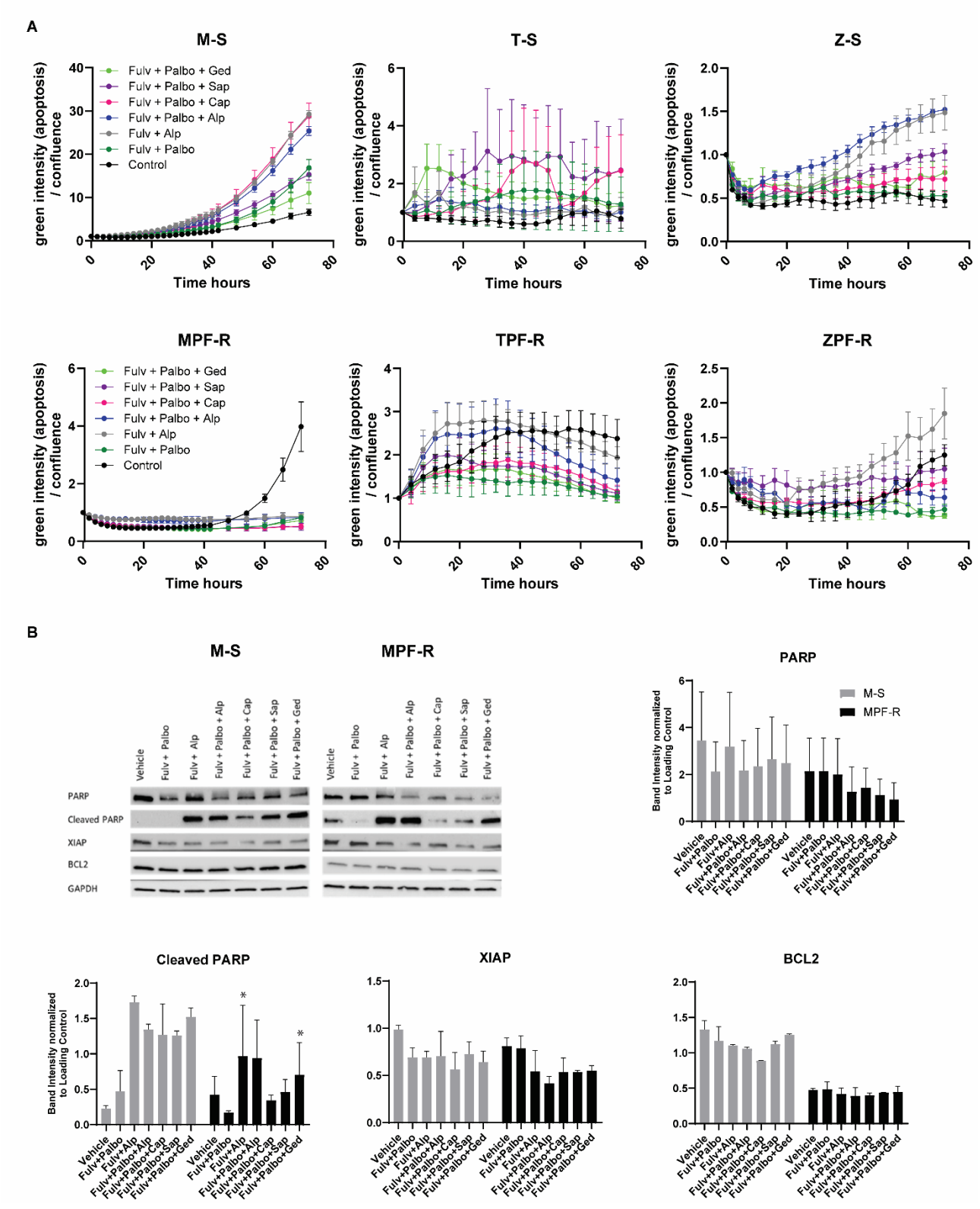

Supplementary Figure S2. Triple combination of inhibitors of the PI3K/AKT/mTOR pathway, CDK4/6i and fulvestrant does not induce apoptosis in combined CDK4/6i and fulvestrant resistant ER+ breast cancer cells. Combined palbociclib- and fulvestrant-resistant cells, MPF-R, TPF-R and ZPF-R, and the corresponding sensitive cells, M-S, T-S and Z-S, were treated with different inhibitors of the PI3K/AKT/mTOR pathway including alpelisib (Alp: 1 µM in M-S/MPF-R, 250-500 nM in T-S/TPF-R; 6 µM

in Z-S/ZPF-R), capivasertib (Cap; 250-500 nM in M-S/MPF-R, 100 nM in T-S/TPF-R and 50 nM in Z-S/ZPF-R), sapanisertib (Sap; 10 nM in M-S/MPF-R and 5 nM in TS/TPFR and Z-S/ZPF-R), gedatolisib (Ged; 10 nM in M-S/MPF-R and T-S/TPF-R and 5 nM in Z-S/ZPF-R) in combination with palbociclib (Palbo; 200 nM) and fulvestrant (Fulv; 100 nM). **A)** Apoptosis assessment by caspase 3/7 green integrated intensity readout for sensitive and resistant cells over 3 days of treatment in a live-cell imaging system (IncuCyte S3). The data represent the mean of three biological replicates ± SEM **B)** Western blotting analysis evaluating the protein expression of cell death-associated markers. GAPDH was used as loading control. **C)** Densitometry analysis of Western blot bands was performed using the Image Lab software from BioRad. Data are shown as mean of two biological replicates ± SEM of the area under the curve (AUC) normalized to loading control. Significant differences are calculated by one-way ANOVA test (* $P < 0.05$). For comparisons where no asterisks are indicated, no statistically significant differences were observed.

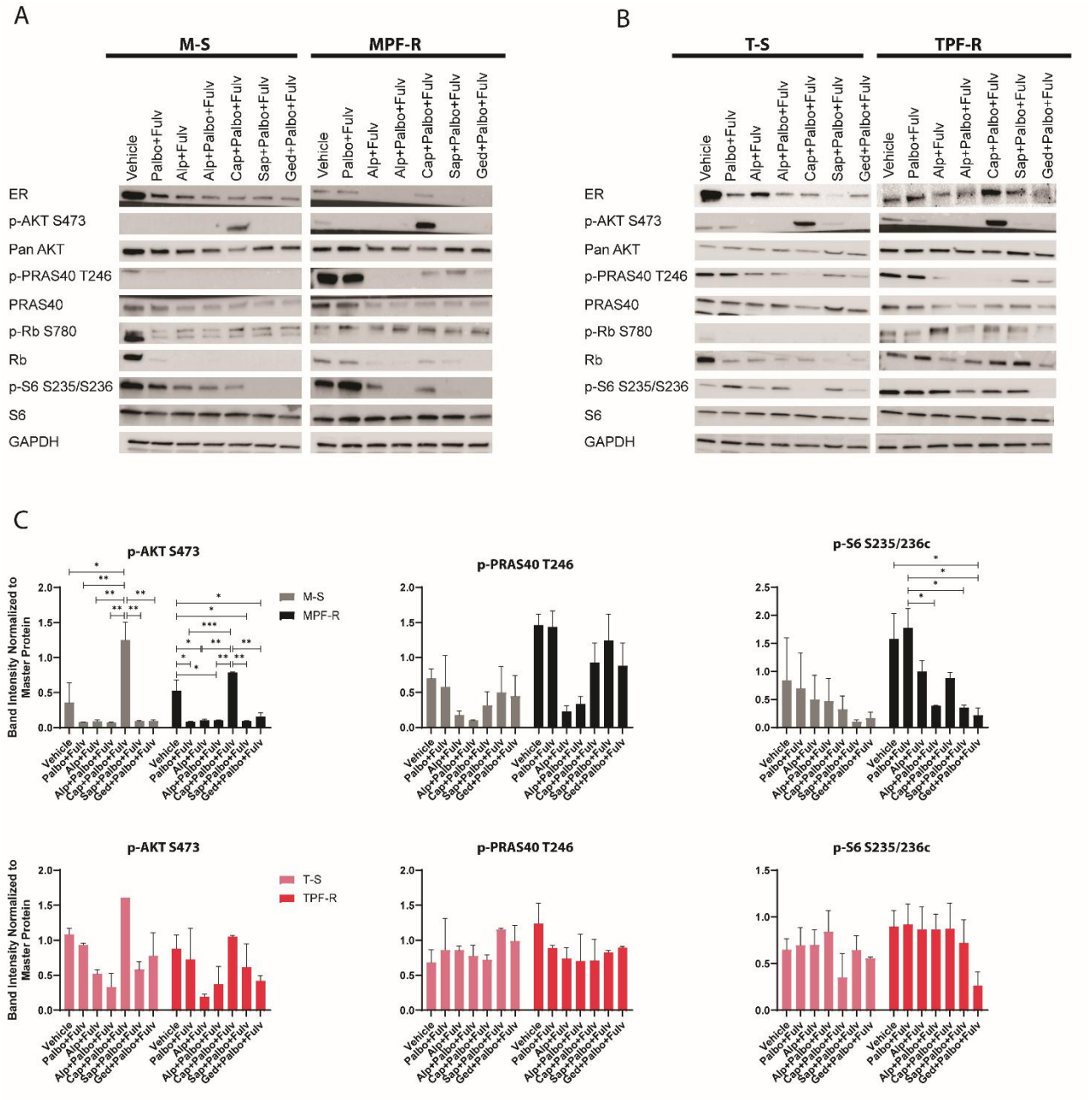

Supplementary Figure S3. Protein levels of key signaling transduction proteins of the PI3K/AKT/mTOR, cyclin D/CDK4-6/Rb and ER pathways. A-B) Cell lysates from the combined palbociclib- and fulvestrant-resistant cells, MPF-R and TPF-R, and corresponding sensitive cells, M-S and T-S, were harvested after 3 days of exposure with the different drug combinations and analyzed using Western blotting with the indicated antibodies. GAPDH was used as a loading control. **C)** Densitometry analysis of Western blot bands was performed using the Image Lab software from BioRad. Data are shown as mean of two biological replicates ± SEM of the AUC normalized to loading control. Significant differences are calculated by one-way ANOVA test (* $P < 0.05$, ** $P < 0.01$ and *** $P < 0.001$). For comparisons where no asterisks are indicated, no statistically significant differences were observed.

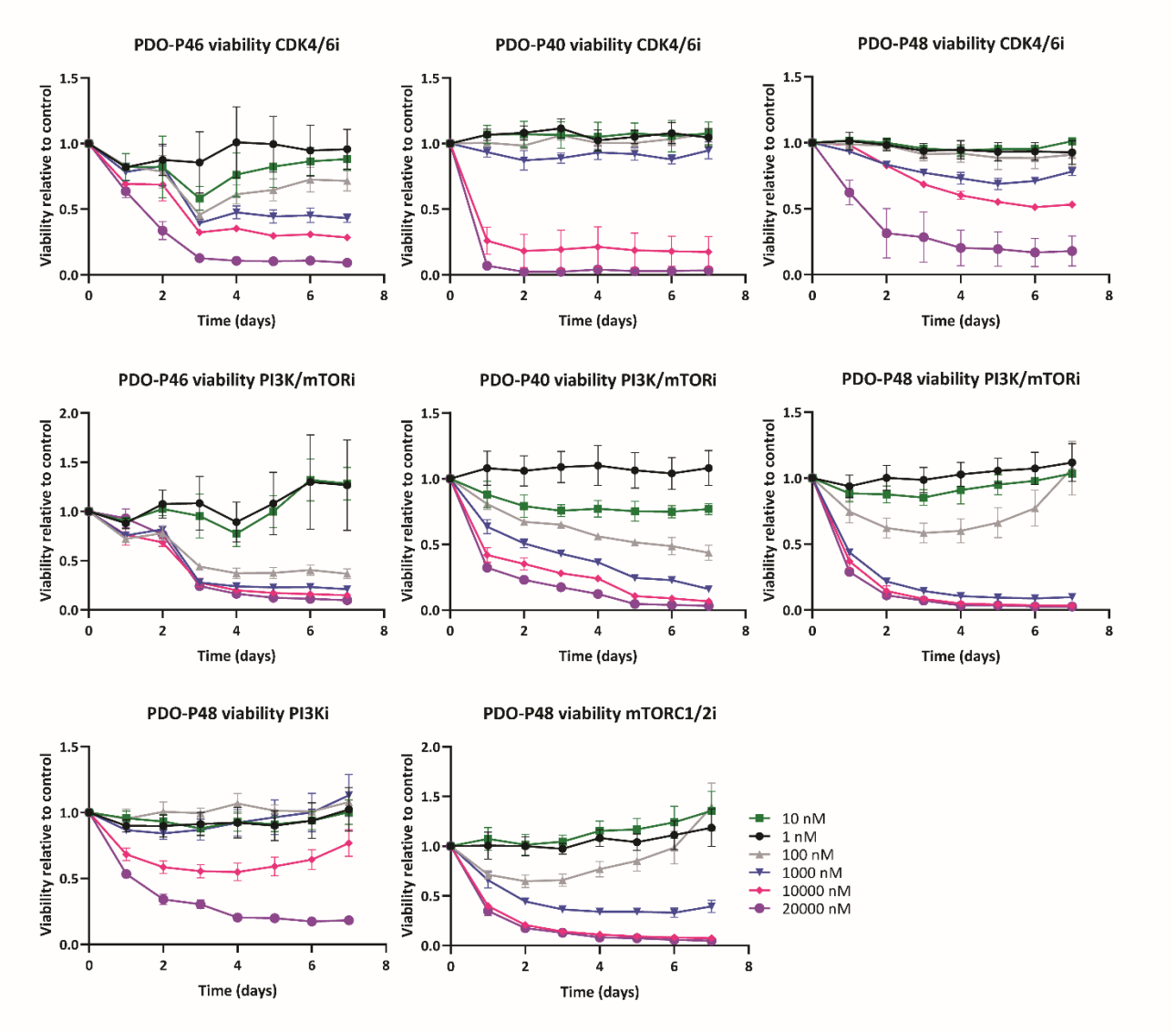

Supplementary Figure S4. Dual PI3K/mTOR inhibitor efficiently reduces viability of ER+ *PIK3CA*- or *AKT1*-mutant breast cancer patient-derived organoids (PDOs) sensitive and resistant to CDK4/6i. Dose-effect curves of CDK4/6i abemaciclib**,** dual PI3K/mTOR inhibitor gedatolisib, PI3Ki alpelisib and dual mTORC1/2i sapanisertib on viability of PDO-P40, PDO-P46 and PDO-P48 during 7 days of treatment. The results represent the mean ± SEMs of three replicates.

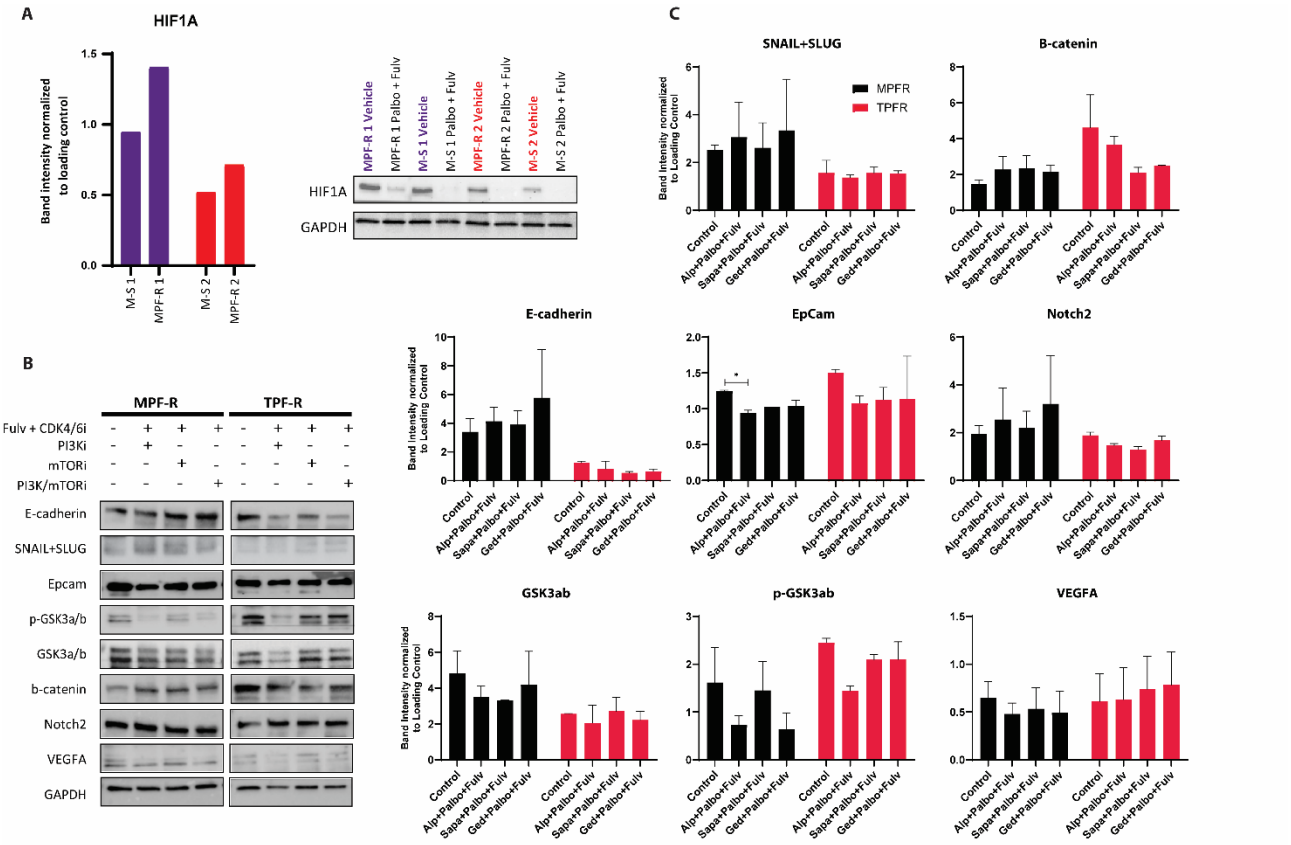

Supplementary Figure S5. Protein levels of key regulators of the EMT, Wnt/β-catenin, hypoxia, and Notch pathways after treatment with triple combination containing single- or dual-node PI3K/mTOR inhibitors. A-B) Cell lysates from the combined palbociclib- and fulvestrant-resistant cells, MPF-R and TPF-R, and corresponding sensitive cells, M-S and T-S, were harvested after 3 days of drug exposure and analyzed using Western blotting with the indicated antibodies. GAPDH was used as a loading control. **C)** Densitometry analysis of Western blot bands was performed using the Image Lab software from BioRad. Data are shown as mean of two biological replicates ± SEM of the AUC normalized to loading control. Significant differences are calculated by one-way ANOVA test (* $P < 0.05$). For comparisons where no asterisks are indicated, no statistically significant differences were observed.

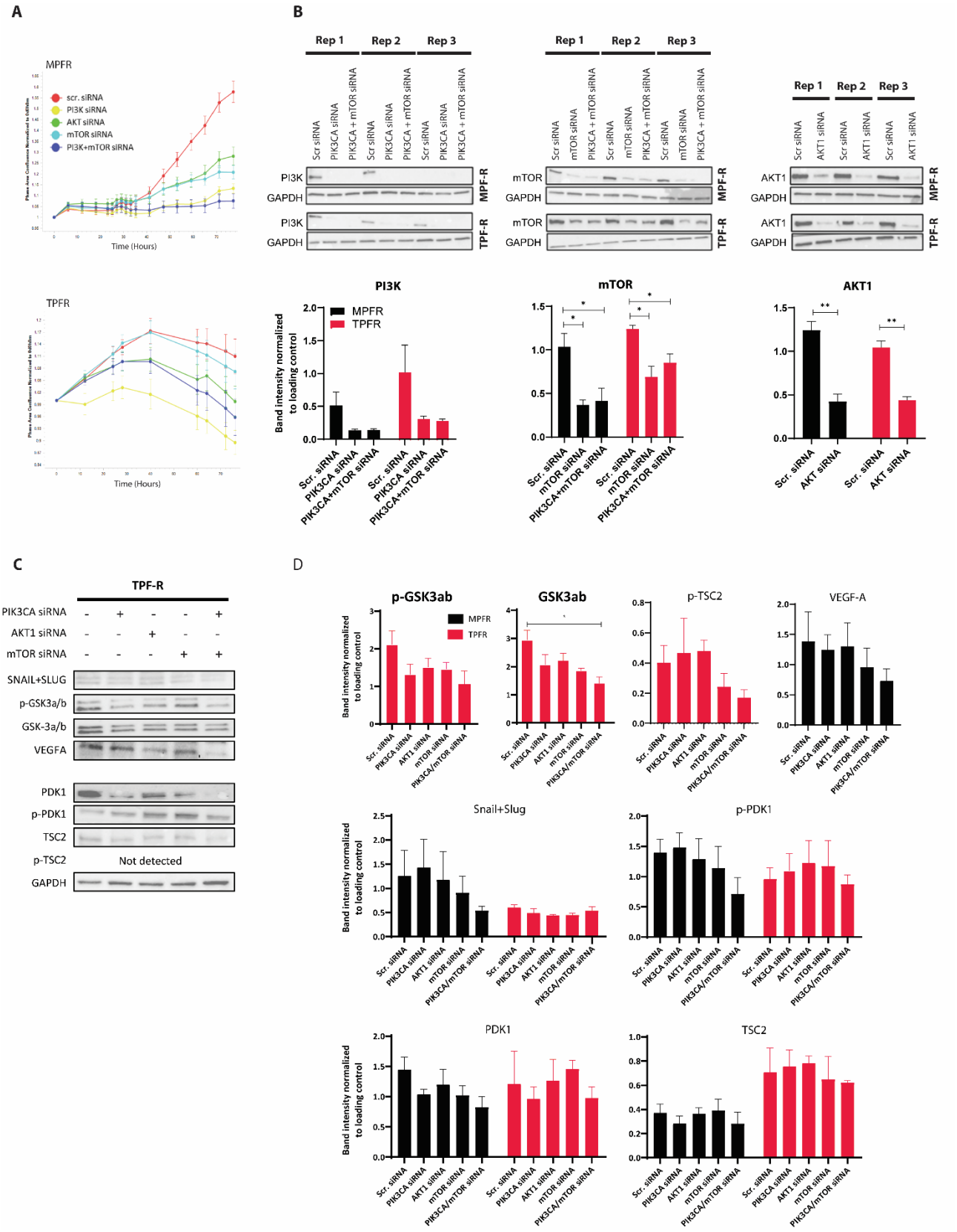

Supplementary Figure S6. Protein levels of key regulators of the EMT, Wnt/β-catenin, hypoxia, and PIK3/AKT/mTOR pathways after siRNA-mediated knockdown of *AKT*, *PIK3CA* or/and *MTOR*. A) Combined palbociclib- and fulvestrant-resistant cells, MPF-R and TPF-R, were treated with specific siRNAs

targeting *AKT*, *PIK3CA* or/and *MTOR*, or control siRNA, and growth was evaluated for 3 days by live-cell imaging (IncuCyte S3). Data are shown as mean ± SEM of phase area confluence normalized to initial confluence (at time 0h). **B-D)** Cell lysates were harvested after 3 days of drug exposure and analyzed using Western blotting with the indicated antibodies. GAPDH was used as a loading control. Densitometry analysis of Western blot bands was performed using the Image Lab software from BioRad. Data are shown as mean of three biological replicates ± SEM of the AUC normalized to loading control. Significant differences are calculated by one-way ANOVA test (* $P < 0.05$ and ** $P < 0.01$). For comparisons where no asterisks are indicated, no statistically significant differences were observed.

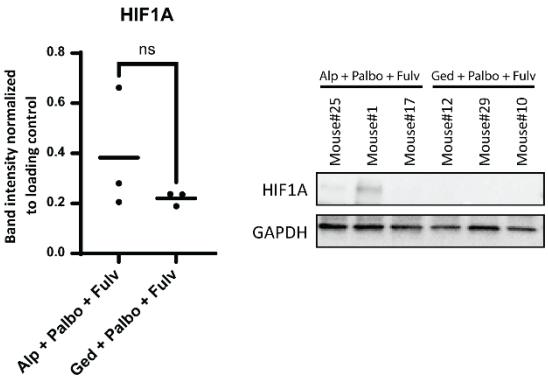

Supplementary Figure S7. HIF-1α expression in *PIK3CA*-mutant ER+ tumor xenografts resistant to combined palbociclib and fulvestrant treated with different triple combinations. Western blot analysis of HIF-1α in 3 xenograft tumors of the alpelisib (Alp+Palbo+Fulv) and gedatolisib (Ged+Palbo+Fulv) treatment groups, excised when mice were sacrificed (from experiment shown in Fig. 3). GAPDH was used as a loading control. Densitometry analysis of Western blot bands was performed using the Image Lab software from BioRad. Data are shown as the AUC normalized to loading control for three biological replicates. Significant differences are calculated by Mann-Whitney U test.

Supplementary Tables

Supplementary Table S1. Expression of cancer stem cell markers after treatment with triple combination containing single PI3Ki compared to triple combination with dual PI3K/mTORi in cells resistant to combined CDK4/6i and endocrine therapy.

Gene Symbol	PI3Ki Avg (log2)	dual PI3K/mTORi Avg (log2)	Fold Change	P-val	FDR P-val
ALDH1A1	4.19	4.29	-1.07	0.5182	0.9393
ALDH1A2	4.68	4.6	1.05	0.9722	0.9992
ALDH1A3	5.83	5.66	1.13	0.0042	0.3427
CD24	11.39	10.92	1.39	0.0201	0.4951
CD44	11.4	10.62	1.72	0.0027	0.3077
NANOG	5.25	5.39	-1.11	0.4595	0.9298
OCT-4	4.89	4.89	1	0.7974	0.9832
SOX2	6.46	6.6	-1.11	0.2112	0.8315

Supplementary Table S2. Gene set enrichment analysis of altered pathways after triple combination with the PI3K inhibitor alpelisib compared to control, by gene expression profiling.

NAME	SIZE	ES	NES	NOM p-val	FDR q-val	FWER p-val	RANK AT MAX	LEADING EDGE
HALLMARK_E2F_TARGETS	186	-0.78606	-3.08615	0	0	0	1517	tags=52%, list=6%, signal=55%
HALLMARK_G2M_CHECKPOINT	182	-0.7656	-2.95952	0	0	0	1331	tags=46%, list=5%, signal=48%
HALLMARK_MTORC1_SIGNALING	193	-0.6314	-2.45943	0	0	0	3506	tags=43%, list=14%, signal=50%
HALLMARK_ESTROGEN_RESPONSE_LATE	191	-0.60774	-2.37623	0	0	0	3262	tags=38%, list=13%, signal=43%
HALLMARK_OXIDATIVE_PHOSPHORYLATION	179	-0.55386	-2.17263	0	0	0	3736	tags=42%, list=15%, signal=49%
HALLMARK_MYC_TARGETS_V2	53	-0.64654	-2.10662	0	0	0	3440	tags=49%, list=14%, signal=57%
HALLMARK_DNA_REPAIR	139	-0.55312	-2.09409	0	0	0	3936	tags=37%, list=16%, signal=43%
HALLMARK_GLYCOLYSIS	192	-0.52732	-2.07062	0	0	0	4954	tags=45%, list=20%, signal=55%
HALLMARK_UNFOLDED_PROTEIN_RESPONSE	100	-0.56119	-1.98885	0	1.65E-04	0.001	4232	tags=39%, list=17%, signal=47%
HALLMARK_MYC_TARGETS_V1	180	-0.51061	-1.98876	0	1.48E-04	0.001	4237	tags=32%, list=17%, signal=38%
HALLMARK_ESTROGEN_RESPONSE_EARLY	193	-0.50115	-1.9792	0	1.35E-04	0.001	5507	tags=42%, list=22%, signal=53%
HALLMARK_MITOTIC_SPINDLE	197	-0.49925	-1.96895	0	1.24E-04	0.001	3249	tags=28%, list=13%, signal=32%
HALLMARK_ADIPOGENESIS	186	-0.4993	-1.92916	0	1.14E-04	0.001	4999	tags=42%, list=20%, signal=53%
HALLMARK_CHOLESTEROL_HOMEOSTASIS	71	-0.55427	-1.88448	0	2.94E-04	0.003	3939	tags=41%, list=16%, signal=48%
HALLMARK_SPERMATOGENESIS	133	-0.48863	-1.84735	0	4.45E-04	0.005	2031	tags=18%, list=8%, signal=20%
HALLMARK_UV_RESPONSE_UP	155	-0.45441	-1.71243	0	0.002067	0.026	3200	tags=32%, list=13%, signal=36%
HALLMARK_PEROXISOME	102	-0.44505	-1.63393	0	0.00551	0.072	2615	tags=25%, list=10%, signal=28%
HALLMARK_PI3K_AKT_MTOR_SIGNALING	102	-0.43095	-1.56388	0.002833	0.011637	0.15	3506	tags=26%, list=14%, signal=31%
HALLMARK_FATTY_ACID_METABOLISM	154	-0.40342	-1.54486	0.001355	0.013518	0.183	3368	tags=29%, list=13%, signal=33%
HALLMARK_REACTIVE_OXYGEN_SPECIES_PATHWAY	46	-0.46527	-1.47029	0.043408	0.027997	0.37	5468	tags=46%, list=22%, signal=58%
HALLMARK_UV_RESPONSE_DN	136	0.409765	1.758129	0	0.002973	0.011	5174	tags=35%, list=20%, signal=43%
HALLMARK_HEDGEHOG_SIGNALING	35	0.411751	1.372438	0.075881	0.058991	0.327	2160	tags=23%, list=9%, signal=25%
HALLMARK_WNT_BETA_CATENIN_SIGNALING	**41**	**0.2913**	**0.975565**	**0.485564**	**0.684379**	**0.999**	**3228**	**tags=15%, list=13%, signal=17%**
HALLMARK_ALLOGRAFT_REJECTION	189	0.209495	0.923647	0.727642	0.663277	1	5070	tags=19%, list=20%, signal=23%

Supplementary Table S3. Gene set enrichment analysis of altered pathways after triple combination with the dual PI3K/mTOR inhibitor gedatolisib compared to control, by gene expression profiling.

NAME	SIZE	ES	NES	NOM p-val	FDR q-val	FWER p-val	RANK AT MAX	LEADING EDGE
HALLMARK_E2F_TARGETS	186	-0.57	-2.3	0	0	0	3383	tags=39%, list=13%, signal=45%
HALLMARK_G2M_CHECKPOINT	182	-0.56	-2.28	0	0	0	5405	tags=49%, list=21%, signal=62%
HALLMARK_ESTROGEN_RESPONSE_LATE	191	-0.56	-2.27	0	0	0	4583	tags=42%, list=18%, signal=51%
HALLMARK_OXIDATIVE_PHOSPHORYLATION	179	-0.56	-2.25	0	0	0	4245	tags=44%, list=17%, signal=52%
HALLMARK_ESTROGEN_RESPONSE_EARLY	193	-0.55	-2.2	0	0	0	4662	tags=38%, list=18%, signal=47%
HALLMARK_MTORC1_SIGNALING	193	-0.54	-2.18	0	0	0	6408	tags=51%, list=25%, signal=68%
HALLMARK_GLYCOLYSIS	192	-0.54	-2.18	0	0	0	4525	tags=41%, list=18%, signal=50%
HALLMARK_CHOLESTEROL_HOMEOSTASIS	71	-0.56	-2.02	0	0	0	3826	tags=38%, list=15%, signal=45%
HALLMARK_UNFOLDED_PROTEIN_RESPONSE	100	-0.53	-1.98	0	0	0	5972	tags=43%, list=24%, signal=56%
HALLMARK_ADIPOGENESIS	186	-0.49	-1.98	0	0	0	5162	tags=41%, list=20%, signal=52%
HALLMARK_DNA_REPAIR	139	-0.49	-1.91	0	0	0.001	6108	tags=47%, list=24%, signal=62%
HALLMARK_MYC_TARGETS_V2	53	-0.54	-1.87	0.001	0.00E+00	0.004	5515	tags=53%, list=22%, signal=67%
HALLMARK_UV_RESPONSE_UP	155	-0.45	-1.8	0	1.00E-03	0.015	4543	tags=38%, list=18%, signal=46%
HALLMARK_P53_PATHWAY	189	-0.43	-1.74	0	2.00E-03	0.02	7002	tags=42%, list=28%, signal=57%
HALLMARK_PI3K_AKT_MTOR_SIGNALING	102	-0.43	-1.61	0.003	0.009	0.1	6588	tags=41%, list=26%, signal=55%
HALLMARK_NOTCH_SIGNALING	**30**	**-0.53**	**-1.59**	**0.021**	**0.009**	**0.114**	**5700**	**tags=40%, list=23%, signal=52%**
HALLMARK_REACTIVE_OXYGEN_SPECIES_PATHWAY	46	-0.47	-1.57	0.007	0.011	0.144	5281	tags=43%, list=21%, signal=55%
HALLMARK_HYPOXIA	**193**	**-0.37**	**-1.51**	**0.001**	**0.019**	**0.251**	**3789**	**tags=25%, list=15%, signal=30%**
HALLMARK_XENOBIOTIC_METABOLISM	190	-0.37	-1.51	0.001	0.019	0.257	4671	tags=27%, list=18%, signal=33%
HALLMARK_MYC_TARGETS_V1	180	-0.37	-1.51	0.002	0.02	0.275	5238	tags=29%, list=21%, signal=36%
HALLMARK_UV_RESPONSE_DN	136	0.278903	1.259822	0.044843	0.208128	0.556	5501	tags=28%, list=22%, signal=36%
HALLMARK_ALLOGRAFT_REJECTION	189	0.195436	0.908378	0.758065	1	1	4335	tags=15%, list=17%, signal=18%
HALLMARK_HEDGEHOG_SIGNALING	35	0.21743	0.76246	0.857534	0.952188	1	2839	tags=17%, list=11%, signal=19%

Supplementary Table S4. Gene set enrichment analysis of altered pathways after triple combination with the dual mTOR inhibitor sapanisertib compared to control, by gene expression profiling.

NAME	SIZE	ES	NES	NOM p-val	FDR q-val	FWER p-val	RANK AT MAX	LEADING EDGE
HALLMARK_E2F_TARGETS	186	-0.71812	-2.85438	0	0	0	2586	tags=53%, list=10%, signal=58%
HALLMARK_G2M_CHECKPOINT	182	-0.70105	-2.80706	0	0	0	2896	tags=50%, list=11%, signal=56%
HALLMARK_MTORC1_SIGNALING	193	-0.61789	-2.4818	0	0	0	3938	tags=45%, list=16%, signal=52%
HALLMARK_ESTROGEN_RESPONSE_LATE	191	-0.60207	-2.43324	0	0	0	3685	tags=41%, list=15%, signal=47%
HALLMARK_GLYCOLYSIS	192	-0.54978	-2.21769	0	0	0	5187	tags=47%, list=20%, signal=59%
HALLMARK_ESTROGEN_RESPONSE_EARLY	193	-0.5492	-2.19614	0	0	0	4037	tags=36%, list=16%, signal=42%
HALLMARK_OXIDATIVE_PHOSPHORYLATION	179	-0.54433	-2.17591	0	0	0	3067	tags=37%, list=12%, signal=42%
HALLMARK_CHOLESTEROL_HOMEOSTASIS	71	-0.60217	-2.11438	0	0	0	4027	tags=44%, list=16%, signal=52%
HALLMARK_ADIPOGENESIS	186	-0.51248	-2.0651	0	0	0	4566	tags=41%, list=18%, signal=49%
HALLMARK_DNA_REPAIR	139	-0.5156	-1.99767	0	0	0	5241	tags=42%, list=21%, signal=53%
HALLMARK_UNFOLDED_PROTEIN_RESPONSE	100	-0.53533	-1.97352	0	0	0	5493	tags=42%, list=22%, signal=53%
HALLMARK_MYC_TARGETS_V2	53	-0.57799	-1.92143	0	2.02E-04	0.002	4683	tags=51%, list=18%, signal=62%
HALLMARK_MYC_TARGETS_V1	180	-0.45591	-1.83138	0	3.70E-04	0.004	4539	tags=30%, list=18%, signal=36%
HALLMARK_UV_RESPONSE_UP	155	-0.45674	-1.78791	0	8.52E-04	0.01	4319	tags=37%, list=17%, signal=44%
HALLMARK_REACTIVE_OXYGEN_SPECIES_PATHWAY	46	-0.51086	-1.66763	0.006309	0.003993	0.045	5278	tags=48%, list=21%, signal=60%
HALLMARK_SPERMATOGENESIS	133	-0.42724	-1.63483	0.00137	0.005467	0.065	4177	tags=24%, list=16%, signal=29%
HALLMARK_MITOTIC_SPINDLE	197	-0.40086	-1.62063	0	0.006081	0.077	4610	tags=34%, list=18%, signal=41%
HALLMARK_P53_PATHWAY	189	-0.40014	-1.58273	0.001318	0.009425	0.124	4849	tags=31%, list=19%, signal=38%
HALLMARK_PI3K_AKT_MTOR_SIGNALING	102	-0.4273	-1.57858	0	0.009456	0.129	5089	tags=32%, list=20%, signal=40%
HALLMARK_PEROXISOME	102	-0.41752	-1.56105	0.00149	0.010178	0.147	2939	tags=25%, list=12%, signal=28%
HALLMARK_UV_RESPONSE_DN	136	0.399263	1.729318	0	0.007381	0.02	1918	tags=18%, list=8%, signal=20%
HALLMARK_EPITHELIAL_MESENCHYMAL_TRANSITION	**193**	**0.2192**	**0.981771**	**0.54185**	**1**	**1**	**4080**	**tags=20%, list=16%, signal=23%**
HALLMARK_ALLOGRAFT_REJECTION	189	0.200506	0.894362	0.789883	1	1	7073	tags=27%, list=28%, signal=37%
HALLMARK_HEDGEHOG_SIGNALING	35	0.260179	0.870221	0.683417	1	1	3285	tags=23%, list=13%, signal=26%
HALLMARK_WNT_BETA_CATENIN_SIGNALING	**41**	**0.223005**	**0.768538**	**0.86579**	**0.946921**	**1**	**177**	**tags=5%, list=1%, signal=5%**

Supplementary Table S5. KEGG and Halmark pathways downregulated in cells treated with triple combination containing dual PI3K/mTORi compared to triple combination containing single PI3Ki, using our phospho-proteomic data.

Enrichment FDR	nGenes	Pathway Genes	Fold Enrichment	Pathway	Genes
0.005409842	4	34	11.03230473	KEGG Circadian rhythm	CREB1 DBP PRKAA1 PRKAA2
3.21E-07	12	106	10.61599134	KEGG Glucagon signaling pathway	CREB1 CREBBP CRTC2 SIRT1 GNAS PDHA1 PDHA2 PRKAA1 PRKAA2 PPP4R3A CAMK2A CAMK2D
0.000392327	7	71	9.245382129	KEGG Adherens junction	CREBBP CTNNB1 ERBB2 AFDN MAPK1 MAPK3 VCL
0.00092018	6	62	9.074960338	KEGG Longevity regulating pathway-multiple species	SIRT1 PRKAA1 PRKAA2 RPS6KB1 AKT1S1 IRS4
2.86E-05	10	109	8.60317341	KEGG HIF-1 signaling pathway	CDKN1B CREBBP ERBB2 PDHA1 PDHA2 MAPK1 MAPK3 RPS6KB1 CAMK2A CAMK2D
0.000867378	7	84	7.81454918	KEGG ErbB signaling pathway	CDKN1B ERBB2 MAPK1 MAPK3 RPS6KB1 CAMK2A CAMK2D
0.000392327	8	101	7.42769031	KEGG Melanogenesis	CREB1 CREBBP CTNNB1 GNAS MAPK1 MAPK3 CAMK2A CAMK2D
0.00092018	7	89	7.375529563	KEGG Longevity regulating pathway	CREB1 SIRT1 PRKAA1 PRKAA2 RPS6KB1 AKT1S1 IRS4
0.001179222	7	95	6.909706644	KEGG Endocrine resistance	CDKN1B ERBB2 GNAS MAPK1 MAPK3 RPS6KB1 SP1
0.001250242	7	97	6.767238465	KEGG Prostate cancer	CDKN1B CREB1 CREBBP CTNNB1 ERBB2 MAPK1 MAPK3
0.000392327	9	131	6.442529095	KEGG Spliceosome	USP39 ACIN1 SF3B1 HNRNPA1 CTNNBL1 SRSF2 SRSF4 SRSF5 SRSF6
0.000392327	9	131	6.442529095	KEGG FoxO signaling pathway	CDKN1B CREBBP SIRT1 PRKAA1 PRKAA2 MAPK1 MAPK3 RBL2 IRS4
0.00092018	8	121	6.199972903	KEGG AMPK signaling pathway	CREB1 CRTC2 SIRT1 PRKAA1 PRKAA2 RPS6KB1 AKT1S1 IRS4
0.000392327	10	155	6.049973559	KEGG Cushing syndrome	CDKN1B CREB1 CTNNB1 GNAS MAPK1 MAPK3 SP1 CAMK2A CAMK2D ASH2L
0.00654693	6	97	5.800490113	KEGG Circadian entrainment	CREB1 GNAS MAPK1 MAPK3 CAMK2A CAMK2D
0.00654693	6	98	5.741301439	KEGG Aldosterone synthesis and secretion	CREB1 GNAS ATP1A1 ATP2B1 CAMK2A CAMK2D
0.00092018	9	155	5.444976203	KEGG mTOR signaling pathway	EIF4B FLCN RICTOR PRKAA1 PRKAA2 MAPK1 MAPK3 RPS6KB1 AKT1S1
0.002728604	8	149	5.034877324	KEGG Adrenergic signaling in cardiomyocytes	CREB1 GNAS ATP1A1 ATP2B1 MAPK1 MAPK3 CAMK2A CAMK2D
0.001974883	10	221	4.243194125	KEGG cAMP signaling pathway	CREB1 CREBBP GNAS AFDN ATP1A1 ATP2B1 MAPK1 MAPK3 CAMK2A CAMK2D
0.004198752	9	202	4.178075799	KEGG Proteoglycans in cancer	CTNNB1 EIF4B ERBB2 PDCD4 MAPK1 MAPK3 RPS6KB1 CAMK2A CAMK2D
1.69E-07	15	200	7.033094262	HALLMARK G2M CHECKPOINT	TOP2A MKI67 RACGAP1 TACC3 CDKN1B INCENP PDS5B TMPO DKC1 ATRX NUMA1 HMGA1 TLE3 NCL SRSF2
0.000208718	11	200	5.157602459	HALLMARK E2F TARGETS	TMPO TOP2A MKI67 RACGAP1 ATAD2 TACC3 SRSF2 ASF1A HMGA1 CDKN1B PDS5B
0.00075519	10	199	4.712290963	HALLMARK MITOTIC SPINDLE	RACGAP1 NUMA1 SPTBN1 TOP2A MAP1S INCENP MARK4 PALLD RICTOR VCL
0.026254566	5	105	4.465456674	HALLMARK PI3K AKT MTOR SIGNALING	MAPK1 AKT1S1 PRKAR2A CDKN1B PRKAA2
0.010746273	7	150	4.376147541	HALLMARK DNA REPAIR	XPC GTF2F1 TAF12 CETN2 APRT IMPDH2 SRSF6
0.011361784	7	161	4.077156094	HALLMARK APOPTOSIS	CDKN1B CREBBP CTNNB1 APP TOP2A PDCD4 ERBB2
0.025299262	6	144	3.90727459	HALLMARK UV RESPONSE DN	CDKN1B ERBB2 CDK13 ATRX ATP2B1 DBP
0.010746273	8	199	3.76983277	HALLMARK MYC TARGETS V1	SET SRSF2 CBX3 PHB2 HNRNPA1 TRIM28 HDGF IMPDH2

Supplementary Table S6. KEGG and Halmark pathways downregulated in cells treated with triple combination containing dual PI3K/mTORi compared to triple combination containing dual mTORi, using our phospho-proteomic data.

Enrichment FDR	nGenes	Pathway Genes	Fold Enrichment	Pathway	Genes
0.028257	2	30	34.66818182	KEGG Citrate cycle (TCA cycle)	PDHA1 PDHA2
0.043797	2	41	25.36696231	KEGG Homologous recombination	BABAM1 ABRAXAS1
0.015435	3	70	22.28668831	KEGG Central carbon metabolism in cancer	ERBB2 PDHA1 PDHA2
0.049128	2	47	22.12862669	KEGG Pyruvate metabolism	PDHA1 PDHA2
0.010848	4	131	15.87855656	KEGG Spliceosome	SRSF4 SRSF5 SRSF6 SNRNP70
0.028091	3	106	14.71762436	KEGG Glucagon signaling pathway	CREB1 PDHA1 PDHA2
0.028091	3	109	14.31255213	KEGG HIF-1 signaling pathway	ERBB2 PDHA1 PDHA2
0.000759	5	200	13.00056818	HALLMARK E2F TARGETS	TMPO RACGAP1 ATAD2 ASF1A PDS5B